A Contraction Argument for Two-Dimensional Spiking Neuron Models

by

Eric Foxall
B.A.Sc., University of British Columbia, 2010

A Thesis Submitted in Partial Fulfillment of the
Requirements for the Degree of

Master of Science

in the Department of Mathematics

A Contraction Argument for Two-Dimensional Spiking Neuron Models

by

Eric Foxall
B.A.Sc., University of British Columbia, 2010

Supervisory Committee

Dr. Rod Edwards, Supervisor
(Department of Mathematics and Statistics)

Dr. Pauline van den Driessche, Supervisor
(Department of Mathematics and Statistics)

Supervisory Committee

Dr. Rod Edwards, Supervisor
(Department of Mathematics and Statistics)

Dr. Pauline van den Driessche, Supervisor
(Department of Mathematics and Statistics)

ABSTRACT

The field of mathematical neuroscience is concerned with the modeling and interpretation of neuronal dynamics and associated phenomena. Neurons can be modeled individually, in small groups, or collectively as a large network. Mathematical models of single neurons typically involve either differential equations, discrete maps, or some combination of both. A number of two-dimensional spiking neuron models that combine continuous dynamics with an instantaneous reset have been introduced in the literature. The models are capable of reproducing a variety of experimentally observed spiking patterns, and also have the advantage of being mathematically tractable. Here an analysis of the transverse stability of orbits in the phase plane leads to sufficient conditions on the model parameters for regular spiking to occur. The application of this method is illustrated by three examples, taken from existing models in the neuroscience literature. In the first two examples the model has no equilibrium states, and regular spiking follows directly. In the third example there are equilibrium points, and some additional quantitative arguments are given to prove that regular spiking occurs.

Contents

List of Tables

List of Figures

ACKNOWLEDGEMENTS

I would like to thank:

Rod Edwards and Pauline van den Driessche, for mentoring, support, encouragement, and patience.

PIMS IGTC, for funding me with a Scholarship.

Chapter 1

Introduction

This thesis is concerned with the analysis of a certain class of neuron models, collectively called the adaptive integrate-and-fire (AIF) model. The main result is a sufficient condition on the model parameters for the global asymptotic stability of regular spiking. The derivations and theorems use calculus and linear algebra, together with results from the theory of ordinary differential equations (ODEs), and from the theory of two-dimensional flows.

The thesis is structured as follows. In Chapter 2 the relevant background in mathematical neuroscience is given. In Section 2.1, the spiking mechanism of individual neurons is described. Sections 2.2 and 2.3 give a history of empirical neuron models, leading up to the AIF model. In Section 2.4 the AIF model is described, and a summary of recent literature on the AIF model is given.

Chapter 3 contains results from the theory of ordinary differential equations that are relevant to the AIF model. The existence, uniqueness and regularity of solutions is discussed, concluding with the variational equation for the flow.

Chapter 4 contains the main result. In Section 4.2 the phase plane for the AIF model is described. In Section 4.3 a method is described for obtaining a transverse local Lyapunov exponent (TLLE) for the flow. Section 4.4 contains the statement and the proof of the main result. Chapter 5 contains examples. Concluding remarks are given in Chapter 6.

Figures are generated with Matlab and with the help of Microsoft Paint.

Chapter 2

Background: Single Neuron Models

2.1 Cell dynamics

Every living cell has a membrane that separates the interior of the cell from its exterior, and is selectively permeable to certain ions; neurons are no exception. Selective permeability means that under certain conditions, some ions move freely across the membrane while others do not. Whenever there is a concentration gradient of one or another type of ion across the membrane (i.e., a difference in the concentration of one or more ion types between the interior and exterior of the cell), there arises a potential difference known as the *membrane potential*. By convention, the membrane potential $v = v_{in} - v_{out}$ is the potential inside the cell minus the potential outside the cell. A negative membrane potential corresponds to a *polarized* cell; when the potential rises (i.e., becomes less negative) the cell is *depolarized*. A neuron at rest is in a polarized state; -70 millivolts is a typical rest potential.

Neurons are known to emit action potentials, or spikes. This corresponds to a sudden depolarization followed by a rapid repolarization. A well-known model developed in the 1950s and named after Hodgkin and Huxley [10] is based on measurements of action potentials in the squid giant axon. Here the model is outlined in simplest terms using the flow of Na^+ (sodium) and K^+ (potassium) ions, although other ion types often have a role in the dynamics; in Hodgkin and Huxley's original model there is an additional leakage current ascribed to Cl^- and other ions. For a more detailed

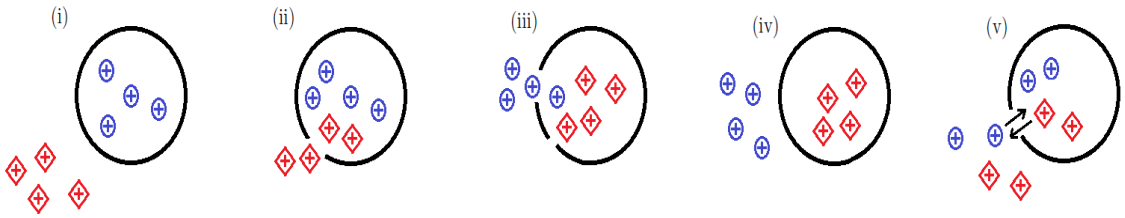

Figure 2.1: Emission of a spike with Na^+ ions (red diamonds) and K^+ ions (blue circles): (i) neuron at rest, channels closed (ii) depolarization, Na^+ channels open (iii) K^+ channels open, Na^+ channels begin to close, repolarization (iv) K^+ channels close (v) sodium potassium pump restores ion concentrations

summary see, for example, [6].

At the interior and exterior of the cell there are Na^+ and K^+ ions (see Figure 2.1). When the neuron is at rest, the concentration of Na^+ is much higher outside the cell than it is inside, and the concentration of K^+ is higher inside the cell. For each ion type there are channels in the membrane that either pass or block the ion depending on their state; we say they are *voltage-gated* channels if their state is voltage dependent. When the neuron is at rest, both its Na^+ and K^+ channels are closed. If the cell becomes somewhat depolarized, both the sodium and potassium channels begin to open. The sodium channels open more quickly, and as Na^+ diffuses into the cell, it further depolarizes the cell, and this gives the steep rise in potential. The sodium channels are transient, however, so that the flow of Na^+ ions is eventually stopped. The potassium channels then have time to catch up, and K^+ ions flood out of the cell and repolarize it, and this gives the sharp drop in potential. A mechanism called the sodium potassium pump then gradually restores the concentration gradient of Na^+ and K^+ ions across the membrane, so that after a (possibly short or possibly long) refractory period the neuron will be ready to spike again. For in-vitro recordings of spiking activity see for example Chapter 8 of [12].

2.2 Simple model

We are interested in modeling the spiking behaviour. The mechanism proposed above by Hodgkin and Huxley, with some important details that are left out here, gives a set of equations that describe the spiking behaviour of a neuron. This is an example

of a *physiological* model, i.e., a model that is based directly on the physical interactions taking place at the cellular level. The Hodgkin-Huxley model is a detailed model, but as a consequence of this detail, it is difficult to analyze mathematically. As we will see, it is possible to capture much of the dynamics using simpler *empirical* models. These are models for which the variables and the parameters may not have a direct physiological interpretation, but that are capable of reproducing one or more important features of the dynamics, and are easier to analyze mathematically.

An example of an empirical model is the following model proposed by Lapicque [14] in 1907. Lapicque models the neuron as a polarizable membrane with an excitation threshold; that is, subject to a sudden change in potential, ions diffuse across the membrane until either equilibrium is restored at a new potential, or the membrane potential reaches the excitation threshold and fires a spike. The polarization assumption leads to a circuit model in which the neuron is modeled by a capacitor and a resistor placed in parallel. Let v denote the threshold potential, then the following equation relates the input V to the spiking time t, with R the input resistance, ρ the cell resistance and K the cell capacitance:

$$v = V\frac{\rho}{R+\rho}(1 - e^{-t\frac{R+\rho}{R\rho K}}) \tag{2.1}$$

Lapicque's interest was in fitting the above equation to observed data. He experimented on the toad sciatic nerve, a nerve that excites the leg muscle, and measured the required duration and strength of the input, fitting the data points to his model with some degree of success. The resulting fit does not constitute, in its own right, a full validation of Lapicque's model, since the model is not used (and indeed could not easily be used, at that time) to simulate the dynamics of the neuron over a significant window of time, or over repeated spiking events. However, it represents a first instance of what has later turned out to be a widely used neuron model.

2.3 Integrate-and-fire model

Lapicque's model gives a description of the neuron's response to a stimulus, and assumes that the neuron spikes when it reaches a certain threshold, but does not model what happens after a spike. An easy way to do this is to add a reset condition:

if v reaches the threshold or spiking potential v_S it is instantaneously reset to a fixed value $v_R < v_S$. Since the repolarization following a spike is quite sharp, this is a fairly good approximation. The idea of a reset appears in the literature as early as the 1930s (see for example Hill, 1936 [9]), and also in the 1960s (see Stein, 1965 [19]). In an important paper in 1972, Knight [13] uses a reset model in the analysis of a network of neurons and gives it the name *integrate-and-fire* (IF) model. In its most general form the IF model is given by

$$v'(t) = f(v, t)$$

with the reset condition $v(t^-) = v_S \Rightarrow v(t^+) = v_R$, where $v(t^-)$ denotes $\lim_{t \to t^-} v(t)$ and $v(t^+) = \lim_{t \to t^+} v(t)$. Differentiating Lapicque's equation and re-writing constants gives the *leaky integrate-and-fire* (LIF) model

$$v'(t) = I(t) - \frac{1}{\tau} v(t)$$

where $' = d/dt$ denotes the time derivative and $I(t)$ is an arbitrary (possibly time-varying) input (the use of the letter I suggests a current, but we will not be too concerned about units; it suffices to note that $I(t)$ is an input signal). The potential $v(t)$ integrates the input $I(t)$ and "leaks out" on a time scale τ.

A sample solution to the LIF model is shown in Figure 2.2. Clearly, the $v(t)$ curve does not exhibit the sharp rise that is typical of a spiking event; in this sense the LIF model models the *subthreshold* dynamics, and not the spiking event itself. In other words, the physical assumption is that once v_S is reached the potential of the neuron rises sharply, spikes and then returns to v_R, so that v_S is the potential at which a spike is initiated, rather than the maximum potential reached during a spike. Despite this shortcoming, as a model of spike timing the LIF model has been found quite effective; a notable example is the phenomenon of mode locking, which is analyzed in [4]. In the presence of a periodic input, $q : p$ locking has been experimentally observed where there are p spiking events for every q input cycles (see for example the references listed in [4]), and aperiodic spiking has also been observed. A depiction of mode locking and of aperiodic spiking is given in Figure 2.3.

Using different forms of the IF model it is possible to obtain a better fit to experimental $v(t)$ curves, that is, to fit not only the observed spike times but also the

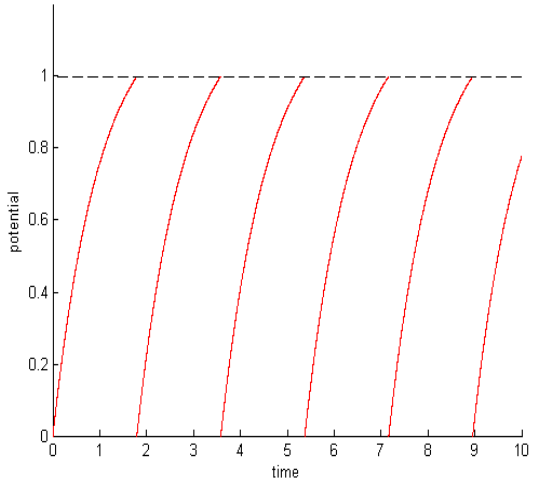

Figure 2.2: Solution of the LIF model with constant input; $v(t)$ curve is shown in red, and the dashed horizontal line corresponds to $v_S = 1$, with $v_R = 0$. Spiking times correspond to values t_S such that $\lim_{t \to t_S^-} v(t) = v_S$, i.e., moments in time such that the curve intersects the dotted line at $v = 1$.

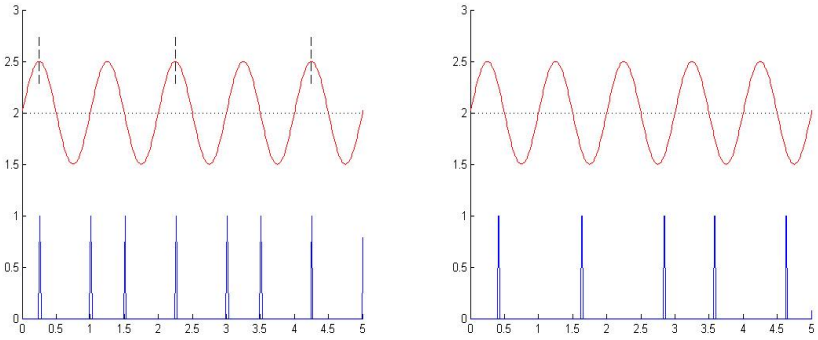

(a) 2:3 mode locking (b) aperiodic spiking

Figure 2.3: Depiction of spiking modes with periodic input above in red and spiking events below in blue

observed shape of the potential curve. For example, the exponential IF model given by

$$v'(t) = e^{v(t)} - v(t) + I(t)$$

has been fitted to experimental potential curves of pyramidal cells [1]. Since the spiking event itself is simulated, in the exponential model the parameter v_S is chosen so that it corresponds to the maximum potential reached during a spike.

2.4 Adaptive model

Higher-order periodic spiking or *bursting* (i.e., any repetitive spiking pattern that takes at least two spiking events to repeat itself) has also been experimentally observed in the absence of a time-varying input. The IF model, however, exhibits either rest (no spiking) or regular spiking (a spiking pattern that repeats itself after each spike) when $I(t)$ is constant. One way to extend the model is to add a second variable, called the adaptation variable and denoted by w. This is one of the simplest ways to extend the model, and as it turns out, this extension alone allows the model to exhibit many biologically realistic behaviours that are not possible in the one-dimensional models so far discussed. An example of such behaviour is refractoriness, in which there is a short period directly following a spike during which the neuron is not able to spike again immediately. To see this, compare the LIF model depicted in Figure 2.2 with the model depicted in Figure 2.4 (a) and (c). In the simulation of the LIF model, the potential begins to increase immediately following a spike, whereas for the other model the potential dips after a spike before increasing again.

A simple two-variable model is given by:

$$\begin{aligned} v' &= F(v) - w + I(t) \\ w' &= a(bv - w) \end{aligned}$$

with $F(v)$ convex, so that v' has a unique minimum, which is usually placed near the resting potential. Note that in Chapter 4 the current $I(t)$ is taken to be a constant. For technical reasons it is also assumed that $F(v)$ is at least C^2, i.e., twice continuously differentiable. If $v(t)$ reaches the spiking potential v_S, then the potential is reset to v_R as in the IF model, and the adaptation variable w is incremented by a positive

constant. In symbolic language this reads

$$v(t^-) = v_S \Rightarrow v(t^+) = v_R,\ w(t^+) = w(t^-) + d$$

for some fixed $d > 0$. A large value of d corresponds to a large refractoriness, which in general leads to a longer delay following a spike and a decreased tendency for bursting. Since the adaptation variable "remembers" what happened after a spiking event, this model is in principle capable of bursting in the presence of a constant input, and this is indeed the case under certain conditions; see for example Figure 2.4 (c) in which there is bursting with two spikes per burst. This class of models is called the *adaptive integrate-and-fire* (AIF) model, and is the subject of the main result of this thesis, which is given in Chapter 4.

The first instance of the AIF model to appear in the neuroscience literature is called the Izhikevich model [11], in which $F(v)$ is quadratic. The model is presented in Ch. 8 of [12] as a simple extension of the IF model. The model is shown to agree both qualitatively and quantitatively with a large number of experimentally observed firing patterns. Figure 2.4 shows the model's reproduction of three important spiking regimes for biological neurons. Note that the Izhikevich model is accurate, but not based on physiological properties in as much detail as the Hodgkin-Huxley model, since the Izhikevich model does not describe the dynamics of ion channels expicitly. Therefore, as observed by Izhikevich, the model is more suitable for large-scale simulations of networks of neurons than it is for determining the spike generation mechanism of any particular neuron. This is a general property of the AIF model.

A second instance of the AIF model is the adaptive exponential integrate-and-fire (aEIF) model, introduced by Brette and Gerstner in [2], in which $F(v)$ takes the form $e^v - v$. In that paper the model is compared to simulated data produced by a more detailed physiological model and close agreement is found. A systematic method of parameter estimation is also described, so that the model can be fitted to experimental data; see [3] for an example of such a quantitative fit.

A third instance of the model, called the quartic model with $F(v) = v^4 + 2av$, is introduced in a paper by Touboul [20]. In that paper the AIF model is introduced in its full generality, i.e., as described at the beginning of this section, and a systematic

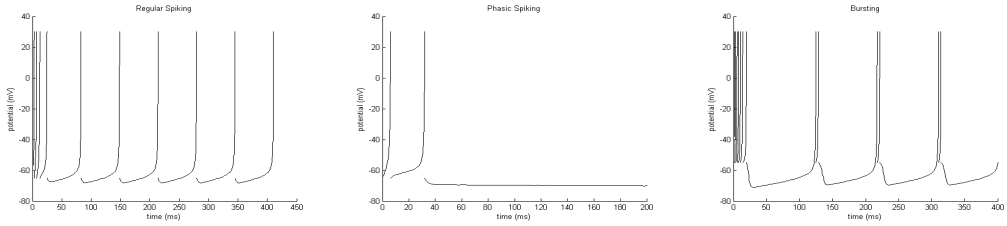

(a) regular spiking (b) phasic spiking (c) bursting

Figure 2.4: Izhikevich model simulation of three biologically important spiking regimes, with time (ms) on the horizontal axis and potential (mV) on the vertical axis. Parameters: $F(v) = 0.04v^2 + 5v + 140$, $a = 0.005$, $b = 0.265$ and $v_S = 30$ in all cases. Regular spiking: $d = 2$, $I = 0$, $w_0 = -20$ (initial value of the adaptation variable) and $v_R = -65$. Phasic spiking: $d = 1.5$, $I = -5$, $w_0 = -25$ and $v_R = -65$. Bursting: $d = 1.5$, $w_0 = -20$, $v_R = -55$, $I = 5$. Initial value of potential set to v_R in all cases.

description is given of the bifurcation structure of the model. Also, the relationship between the bifurcation structure of the model and the various neurocomputational behaviours exhibited by the Izhikevich model and partially depicted in Figure 2.4 is described. The Izhikevich and aEIF models are shown to possess the same bifurcation structure, and the quartic model is shown to exhibit all bifurcations possible in the general AIF model. In particular, the quartic model supports subthreshold oscillations, that is, sustained oscillations that do not lead to spiking, a behaviour that does not occur in either the Izhikevich or the aEIF models.

Further analytical work includes a paper specific to the aEIF model [21]. The bifurcation structure and the subthreshold dynamics, i.e., the dynamics in the absence of spikes, are described. A discrete map called the adaptation map, that encodes information about the spike patterns produced by the model, is also introduced. Parameter values corresponding to certain spiking regimes, such as regular/tonic spiking, bursting, and phasic spiking as depicted in Figure 2.4, can be classified according to the behaviour of the adaptation map; this is described in greater detail in Chapter 4. It is also shown that the adaptation map possesses dense orbits for some parameter values, i.e., that chaotic behaviour is possible for the model. In a subsequent paper [22] Touboul and Brette generalize the analysis to the AIF model and prove several results about the adaptation map, relating it to the spiking dynamics of the model.

Chapter 3

Background: Ordinary Differential Equations in $\mathbb{R}^2$

The main result of this thesis concerns the AIF model, which was introduced in Section 2.4 of the previous chapter. In this chapter we examine solutions to the continuous dynamics of the model. We establish the existence, uniqueness and regularity of solutions. The results given in this chapter are adapted from [16] to fit the context of the AIF model.

3.1 Continuous dynamics of the AIF model

The continuous dynamics of the AIF model take the form

$$\begin{aligned} v' &= f(v,w) \\ w' &= g(v,w) \end{aligned} \tag{3.1}$$

where $f(v,w) = F(v) - w + I$, $g(v,w) = a(bv - w)$ and $' = d/dt$ denotes the time derivative. The input current I is here taken to be a constant. A solution of the model is a pair of functions $(v(t), w(t))$ defined for t in some interval and satisfying the relations in (3.1). Given the state (v_0, w_0) at time τ a natural question is the existence and uniqueness of a solution satisfying $v(\tau) = v_0$ and $w(\tau) = w_0$. This is called the initial value problem. Uniqueness can be stated as follows: if $(v_1(t), w_1(t))$ and $(v_2(t), w_2(t))$ are two solutions that satisfy the same initial condition, then $v_1(t) = v_2(t)$ and $w_1(t) = w_2(t)$ for all t for which both solutions are

defined. For a model of a physical system, existence and uniqueness of solutions is clearly a desirable feature.

Solutions live in state space, which is the space containing all possible states of the system. In the present setting, the state space is two-dimensional and is often called the phase plane. For efficiency of notation, the time derivatives v' and w' are gathered into the function $X(v,w) = (v', w') = (f(v,w), g(v,w))$. A solution is then a function $\phi : J \to \mathbb{R}^2$ that maps a non-degenerate interval J (i.e., an interval that contains an open set) into the phase plane and satisfies $\phi'(t) = X(\phi(t))$ for each $t \in J$. Given (τ, x) in $\mathbb{R} \times \mathbb{R}^2$, the initial value problem is to find a solution defined on an open set containing τ and for which $\phi(\tau) = x$. The function X is called the vector field since it can be pictured as a family of vectors on the phase plane that specifies the velocity of a solution at each point. In order to have a fixed (time-independent) vector field it is necessary that v' and w' have no explicit time dependence.

3.2 Definitions

In order to make the discussion more general the vector field is defined not necessarily on all of $\mathbb{R}^2$ but on a *domain* D, that is, an open connected subset of $\mathbb{R}^2$. Before addressing solutions of the model, a few definitions are required. Let f be a function that maps a subset U of $\mathbb{R}^n$ into a subset V of $\mathbb{R}^m$, for positive integers n and m.

Definition 3.2.1. *A function f is said to be C^k with respect to the variables $(x_1, x_2, ..., x_n)$ if each of the partial derivatives $\partial_{\alpha_1}\partial_{\alpha_2}...\partial_{\alpha_m} f$ exists and is continuous, where $0 \leq m \leq k$, and each α_i is equal to some x_j.*

If f is C^k with respect to $x_1, ..., x_n$ at each point in U the notation $f \in C^k(U, V)$ is used. If f is continuous the notation $f \in C(U, V)$ is used.

Definition 3.2.2. *A function f satisfies a* Lipschitz condition *on a set $S \subset U$ with Lipschitz constant $L > 0$ if $x, y \in S$ implies $|f(x) - f(y)| \leq L|x - y|$. f is* Lipschitz *if it satisfies a Lipschitz condition on any bounded subset of U.*

A Lipschitz condition is stronger than continuity; it gives a uniform bound on the slope of the line that joins two points on the graph of the function. For example, $f(x) = \sin x$ satisfies a Lipschitz condition since its slope never exceeds 1 in absolute

value. On the other hand, $f(x) = \sqrt{x}$ does not satisfy a Lipschitz condition on its domain, since its slope tends to ∞ as x approaches zero from the right. An important property of Lipschitz functions is given below.

Lemma 3.2.3. *If f is Lipschitz, then $|f|$ is bounded on any bounded subset of its domain.*

Proof. Let S be a bounded set and let $M > 0$ be such that $|x| < M$ for all $x \in S$. Let L be a Lipschitz constant for f on S. Then $x, y \in S$ implies $|f(x) - f(y)| \leq L|x - y| \leq 2LM$. Take $y \in S$, then $|f(x)| \leq |f(y)| + 2LM$ for all $x \in S$. In particular, $|f|$ is bounded on S. □

3.3 Existence and uniqueness of solutions

In the results that follow X is assumed to be Lipschitz. The first theorem gives an affirmative answer to the question of existence and uniqueness for the initial value problem.

Theorem 3.3.1 (Cauchy-Lipschitz)**.** *Let $(\tau, x) \in \mathbb{R} \times D$. Then there is an open interval J containing τ and a unique function $\phi \in C^1(J, D)$ that satisfies $\phi(\tau) = x$ and $\phi'(t) = X(\phi(t))$ for each $t \in J$.*

The function ϕ is called a local solution since it is defined on a small open interval containing τ. Observe that ϕ solves the initial value problem with initial value (τ, x). Note the following invariance of solutions.

Proposition 3.3.2. *Let ϕ be a solution defined on an interval J. For $s \in \mathbb{R}$, the function ψ defined by $\psi(t) = \phi(t - s)$ is a solution on the interval $\{t : t - s \in J\}$.*

Proof. $\psi'(t) = \phi'(t - s) = X(\phi(t - s)) = X(\psi(t))$ and $t - s \in J$ implies that $\phi(t - s)$, and therefore $\psi(t)$, are well-defined. □

This property is called translation invariance, or sometimes time-shift invariance. It relies on the fact that X has no explicit time dependence.

The Cauchy-Lipschitz theorem gives uniqueness of the local solution. The following result extends uniqueness to solutions defined on arbitrary intervals.

Lemma 3.3.3. *For $\tau \in \mathbb{R}$ let ϕ and ψ be solutions defined on intervals J and J' both containing τ, and suppose $\phi(\tau) = \psi(\tau)$. Then $\phi(t) = \psi(t)$ for $t \in J \cap J'$.*

Proof. Let J'' denote $J \cap J'$. Suppose the set $C = \{t > \tau \in J'' : \phi(t) \neq \psi(t)\}$ is non-empty, and let s denote its infimum. Since solutions are continuous and $\phi(t) = \psi(t)$ for $0 < s - t < \epsilon$ with $\epsilon > 0$ arbitrarily small it follows that $\phi(s) = \psi(s)$. Let x denote this common value. Since $s = \sup\{J''\}$ is impossible, let $\delta > 0$ be such that $[s, s+\delta) \in J''$. By the Cauchy-Lipschitz theorem there is a unique solution γ defined on an open interval containing s and satisfying $\gamma(s) = x$. Since ϕ and ψ are both solutions this implies that $\phi(t) = \psi(t)$ for t in an open interval that contains s. Since this is a contradiction, it follows that C is empty. Applying the same argument to the set $\{t < \tau \in J'' : \phi(t) \neq \psi(t)\}$ with the obvious modifications establishes the result. □

3.4 Domain of definition of solutions

At this point it is natural to ask about the largest interval on which a solution is defined. This question is answered in a few steps.

Definition 3.4.1. *Let ϕ be a solution defined on an interval J. A solution ψ is an* extension *of ϕ if ψ is defined on the larger interval $J' \supset J$ and $\psi(t) = \phi(t)$ for $t \in J$.*

A solution defined on a compact interval can always be extended, as shown in the following lemma.

Lemma 3.4.2. *Let ϕ be a solution defined on an interval $[a, b]$, where $-\infty < a, b < \infty$. Then ϕ has an extension to an open interval containing $[a, b]$.*

Proof. Necessarily $\phi(b) \in D$. Let $x = \phi(b)$, then by the Cauchy-Lipschitz theorem, for some $\delta > 0$ there exists a function $\psi(t)$ that satisfies $\psi(b) = x$ and $\psi'(t) = X(\psi(t))$ for t on the interval $(b - \delta, b + \delta)$. Extend ϕ by setting $\phi(t) = \psi(t)$ for $b < t < b + \delta$. Then ϕ is a solution defined on $[a, b+\delta)$. The same argument applies to the left-hand endpoint a. It follows that ϕ is defined on an open interval containing $[a, b]$. □

Definition 3.4.3. *Let ϕ be a solution defined on an interval J. The* maximal interval *for ϕ is the union of all intervals J' such that ϕ has an extension to J'. If ϕ is defined on its maximal interval then it is said to be non-extendable.*

The preceding lemma implies that the maximal interval is open. For the next two results assume ϕ is a solution defined on an interval (a, b). If for each $M > 0$ there exists ϵ such that $b - \epsilon < t < b$ implies $|\phi(t)| > M$, the notation $\lim_{t\to b^-} \phi(t) = \infty$ is used. In this context ∞ is thought of as the "point at infinity".

Lemma 3.4.4. *Suppose* $\limsup_{t\to b^-} |\phi(t)| = \infty$. *Then* $\lim_{t\to b^-} \phi(t) = \infty$.

Proof. Suppose there exists a sequence $s_n \to b$ with $\limsup |\phi(s_n)| = M < \infty$. Let $S = \{x \in D : |x| < 2M\}$ and let L be a Lipschitz constant for X on S. For $\epsilon > 0$, take n so that $b - \epsilon < s_n < b$. Let $c = \inf\{s_n < t < b : |\phi(t)| > 2M\}$; for ϵ small enough this is non-empty by assumption, and $|\phi(c)| = 2M$ by continuity of ϕ. By the mean value theorem there exists d with $s_n < d < c$ and $\phi'(d) = (\phi(c) - \phi(s_n))/(c - s_n)$. Since $|\phi(s_n)| \leq M$ it follows that $|X(\phi(d))| = |\phi'(d)| \geq M/\epsilon$. But ϵ is arbitrary and by choice of c, $\phi(d)$ lies in S, so that X is unbounded on S. Since X is Lipschitz and S is bounded this is impossible. Therefore, $s_n \to b$ implies $\limsup |\phi(s_n)| = \infty$, and the result follows. □

Lemma 3.4.5. *The limits* $\lim_{t\to b^-} \phi(t)$ *and* $\lim_{t\to a^+} \phi(t)$ *both exist, and may be equal to* ∞.

Proof. Suppose $\limsup_{t\to b^-} |\phi(t)| = M < \infty$; the other case is already proved. Let S be defined as in the last proof and let P be a bound for $|X|$ on S. Let $s_n \to b$, then (s_n) is a Cauchy sequence. For $\epsilon > 0$ let N be such that $n, m \geq N$ implies $|s_n - s_m| < \epsilon/(2P)$. For $s_n < s_m$, apply the mean value theorem to find that $\phi(s_n) - \phi(s_m) = \phi'(c)(s_n - s_m) = X(\phi(c))(s_n - s_m)$ for some c with $s_n < c < s_m$. For n, m large enough, $\phi(c) \in S$, so that $|\phi(s_n) - \phi(s_m)| \leq P|s_n - s_m| \leq P\epsilon/(2P) < \epsilon$ and $(\phi(s_n))$ is a Cauchy sequence. Therefore $(\phi(s_n))$ converges. Let (s_n) and (t_n) each be sequences with limit b, then by interlacing s_n and t_n it can be shown that $(\phi(s_n))$ and $(\phi(t_n))$ have the same limit. It follows that $\lim_{t\to b^-} \phi(t)$ is well-defined. A similar argument shows that $\lim_{t\to a^+} \phi(t)$ exists. □

For $x \in \mathbb{R}^2$ define $|x - D| = \inf\{|x - y| : y \in D\}$. Since D is an open set, the set $\{x \in \mathbb{R}^2 \setminus D : |x - D| = 0\}$ gives the boundary of D, and is denoted ∂_D. If D is unbounded the point at infinity is included in ∂D. The following result gives a characterization of non-extendable solutions.

Theorem 3.4.6. *Let* ϕ *be a non-extendable solution and let* (a, b) *denote its maximal interval. Then* b *satisfies one or both of*

1. $\lim_{t\to b^-} \phi(t) \in \partial D$,

2. $b = \infty$.

A similar statement applies to the endpoint a.

Proof. Consider the right-hand endpoint b. If $b = \infty$ there is nothing to prove, therefore suppose $b < \infty$. If $\limsup_{t\to b^-} |\phi(t)| = \infty$ then by Lemma 3.4.4, $\lim_{t\to b^-} \phi(t) = \infty$, which by definition is included in ∂D. Otherwise, $\lim_{t\to b^-} \phi(t)$ exists and is not equal to ∞. Let c denote this limit; clearly $|c - D| = 0$. If $c \in D$ then ϕ is defined on $(a, b]$, which is a contradiction. Therefore $c \in \partial D$. A similar argument applies to the endpoint a. □

It is possible in the above theorem that both statements hold true, for example if a solution goes to ∞ at a constant speed. It is also possible to have a or b finite. A one-dimensional example is $y' = 1 + y^2$, for which $y(t) = \tan(t)$ is a solution that blows up at $t = \pm\pi/2$.

3.5 Regularity of solutions

Having described individual solutions, the next question is how nearby solutions relate to one another. To assist in this task, the following estimation result is helpful. This is a special case of a well-known result due to Gronwall.

Lemma 3.5.1. *Suppose $v : [a, b] \to \mathbb{R}$ satisfies $v(t) > 0$ for $t \in [a, b]$ and $v(t) \leq v(a) + L\int_a^t v(s)ds$ for some $L > 0$ and for each $t \in [a, b]$. Then $v(t) \leq v(a)e^{L(t-a)}$ on $[a, b]$.*

Proof. Take the derivative to find that $v'(t) \leq Lv(t)$. Divide by $v(t)$ to obtain $\frac{d}{dt}\log v(t) = v'(t)/v(t) \leq L$. Integrate to find that $\log v(t) - \log v(a) \leq L(t - a)$ or $v(t) \leq v(a)e^{L(t-a)}$. □

Surprisingly, the above result is sufficient to establish continuity of solutions with respect to the initial value, and also the existence of nearby solutions. Observe that a solution ϕ defined on an interval J satisfies $\phi(t) = \phi(a) + \int_a^t X(\phi(s))ds$ for each $a, t \in J$, simply by integrating the relation $\phi'(t) = X(\phi(t))$.

Lemma 3.5.2. *Let ϕ be a solution defined on an interval $[a,b]$ with $-\infty < a, b < \infty$, and let $x = \phi(a)$. Then for each $\epsilon > 0$ there is a $\delta > 0$ so that $|y - x| < \delta$ implies the existence of a solution ψ defined on $[a,b]$ and satisfying $\psi(a) = y$ and $|\psi(t) - \phi(t)| < \epsilon$ for $t \in [a,b]$.*

Proof. Let $C = \phi([a,b])$. Since $[a,b]$ is compact and ϕ is continuous, C is compact. Take $\epsilon > 0$ so that the set $U = \{y : |y - C| < \epsilon\}$ is contained in D. Let L be a Lipschitz constant for X on U and let $0 < \delta < \frac{\epsilon}{2} e^{-L(b-a)}$. Take y such that $|y - x| < \delta$. Then $y \in D$, and by the Cauchy-Lipschitz theorem there exists a solution ψ defined on $[a,c)$ for some $c > a$ and satisfying $\psi(a) = y$. Let $c \in [a,b]$ be the largest such value. Using the above integral relation, as well as the triangle inequality and monotonicity of integration, $|\phi(t) - \psi(t)| \leq |y - x| + \int_a^t |X(\phi(s)) - X(\psi(s))| ds$ for $t \in [a,c)$. Using the Lipschitz condition, $|\phi(t) - \psi(t)| \leq |y - x| + L \int_a^t |\phi(s) - \psi(s)| ds$. Applying Gronwall's inequality gives $|\phi(t) - \psi(t)| \leq |y - x| e^{L(t-a)}$. By choice of y, $|\phi(t) - \psi(t)| \leq \delta e^{L(t-a)}$, so that $\psi(t) \in U$ for $t \in [a,c)$ and $\lim_{t \to c^-} \psi(t) \in U$. Therefore, ϕ has an extension to the interval $[a,c]$, and since the maximal interval is open it has an extension to $[a,d)$ for some $d > c$. If $c < b$ this is a contradiction, therefore $c = b$. □

For the solution given in the Cauchy-Lipschitz theorem let $J(\tau, x)$ denote its maximal interval, and let $\phi(t, \tau, x)$ denote the corresponding non-extendable solution. Then $\phi(t, \tau, x)$ is defined for $t \in J(\tau, x)$ and satisfies $\phi(\tau, \tau, x) = x$, $\partial_t \phi(t, \tau, x) = X(\phi(t, \tau, x))$ for each $t \in J(\tau, x)$. The set $S = \{(t, \tau, x) : \tau \in \mathbb{R}, x \in D, t \in J(\tau, x), \}$ describes the largest subset of $\mathbb{R} \times \mathbb{R} \times D$ on which solutions exist, and for this reason $\phi(t, \tau, x)$ is called the *general solution* of the model corresponding to the vector field X. By translation invariance (Proposition 3.3.2), $(t, \tau, x) \in S$ implies $(t - s, \tau - s, x) \in S$ for each $s \in \mathbb{R}$. The general solution also has the following important property.

Theorem 3.5.3. $\phi \in C(S, D)$.

Proof. To show that ϕ is continuous it suffices to do so in each variable. Continuity with respect to t follows from differentiability with respect to t. Continuity with respect to τ follows from continuity with respect to t and translation invariance. To show continuity with respect to x let $(t, \tau, x) \in S$. Continuity with respect to the initial value implies that for each $\epsilon > 0$ there is a $\delta > 0$ such that $|y - x| < \delta$ implies $|\phi(t, \tau, y) - \phi(t, \tau, x)| < \epsilon$. □

The following theorem gives additional regularity of the general solution, whenever X has additional regularity. For $x = (x_1, x_2)$ and $\phi = (\phi_1, \phi_2)^\top$, $X = (X_1, X_2)^\top$,

$\partial_x \phi$ denotes the matrix of partial derivatives $\partial_{x_j} \phi_i$ and DX the matrix of partial derivatives $\partial_{x_j} X_i$, for $1 \leq i, j \leq 2$.

Theorem 3.5.4 (Differentiability of solutions)**.** *Suppose $X \in C^1(D, \mathbb{R}^2)$. Then $\phi \in C^1(S, D)$ and for fixed (τ, x), $\partial_x \phi$ satisfies the linear system*

$$\begin{aligned} \frac{d}{dt} \partial_x \phi(t, \tau, x) &= DX(\phi(t, \tau, x)) \partial_x \phi(t, x) \\ \partial_x \phi(\tau, \tau, x) &= I_2 \end{aligned}$$

where I_2 denotes the 2×2 identity matrix.

The above linear system is called the variational equation for solutions. The proof can be found in [16, Theorem 7.1].

Chapter 4

Main Result

4.1 Background

We recall the definition of the AIF model from Chapter 2:

$$\begin{aligned} v' &= F(v) - w + I \\ w' &= a(bv - w) \end{aligned} \tag{4.1}$$

Here v corresponds to the potential of a neuron, and w is called the adaptation variable. We assume that F is at least C^2, strictly convex, and $F'(v)$ goes to a negative limit as $v \to -\infty$ and to infinity as $v \to +\infty$. The quantity $I \in \mathbb{R}$ is a constant input current, and a and b are positive real parameters. Also, there is the following reset condition: given additional parameters $d > 0$, v_S and v_R, if $t_S \in \mathbb{R}$ is such that $v(t_S^-) = v_S$ then $v(t_S^+) = v_R$ and $w(t_S^+) = w(t_S^-) + d$, where $v(t_S^\pm) = \lim_{t \to t_S^\pm} v(t)$ and similarly for w. In other words, solutions $(v(t), w(t))$ satisfy the ordinary differential equations (ODEs) in (4.1), except when $v(t) \to v_S$, at which time the potential is instantaneously reset to the value v_R, and the adaptation variable w is incremented by the fixed amount d. In the phase plane, the vertical line $\{(v, w) : v = v_R\}$ is the *reset line*, and the vertical line $\{(v, w) : v = v_S\}$ is the *spiking line*. The event $v(t) \to v_S$ is called *spiking*, and the time t_S at which this occurs is the *spike time*. In general $v_S > v_R$ and v_S is fairly large, so that a spike corresponds to a large increase in the potential followed by a sudden drop. In what follows, models of this form are collectively referred to as "the model".

We are primarily interested in the spiking dynamics of the model, that is, the

pattern of spikes produced by solutions of the model. Since the input I is assumed constant, the model is autonomous. Moreover, after each spike the potential is reset to the same value, and the adaptation variable is simply incremented by a constant. As observed in [22], the behaviour of a solution following a spike depends entirely on the value of the adaptation variable at spike time; we recall the following definition.

Definition 4.1.1. *[22, Definition 2.3] Denote by $\mathscr{D}$ the set of adaptation values w_0 such that the solution of* (4.1) *with initial condition (v_R, w_0) reaches v_S in finite time. Let $w_0 \in \mathscr{D}$, and denote by $(v(t), w(t))$ the solution of* (4.1) *with initial condition (v_R, w_0). Let t_S be the first time that $v(t_S^-) = v_S$. The* adaptation map Φ *is then the unique function such that*

$$\Phi(w_0) = w(t_S^-) + d$$

Intuitively, Φ maps the adaptation value following one spike to the adaptation value following the next spike, if another spike occurs (see Figure 4.1). Moreover, the orbit of the adaptation variable under the map Φ gives the spiking behaviour of a solution. For example, if after some number of iterations the adaptation value lands outside the domain of Φ, then the solution ceases to spike. If the adaptation value approaches a fixed point, then the solution ends up in a *regular* spiking pattern. If the adaptation value is attracted to a periodic orbit of period p, then the solution ends up in a periodic spiking or *bursting* pattern, with p spikes per burst. Aperiodic behaviour is also possible, in which spikes are emitted at irregular intervals and do not settle into a predictable pattern. These facts, and examples, are detailed in [22].

We are interested in conditions on the model parameters for global asymptotic stability of regular spiking, i.e., global asymptotic stability of a fixed point for Φ. We address the simplest case $\mathscr{D} = \mathbb{R}$, i.e., every initial condition on the reset line leads to the emission of infinitely many spikes. In [22] it is proved that Φ has a fixed point in this case and is at least continuously differentiable. Therefore, if Φ is *non-expansive*, i.e., $|\Phi'(w)| < 1$ for almost every $w \in \mathbb{R}$, then all orbits converge to a unique fixed point. This follows from the existence of a fixed point p and from the fact that $|\Phi(w) - p| \leq \int_p^w |\Phi'(\zeta)| d\zeta$.

Now, the adaptation map is determined by the orbits, i.e., the paths traced out by trajectories in phase space. If orbits converge then Φ is non-expansive, and if orbits separate then it is possible that $|\Phi'| > 1$. A method described in [15] gives a sufficient

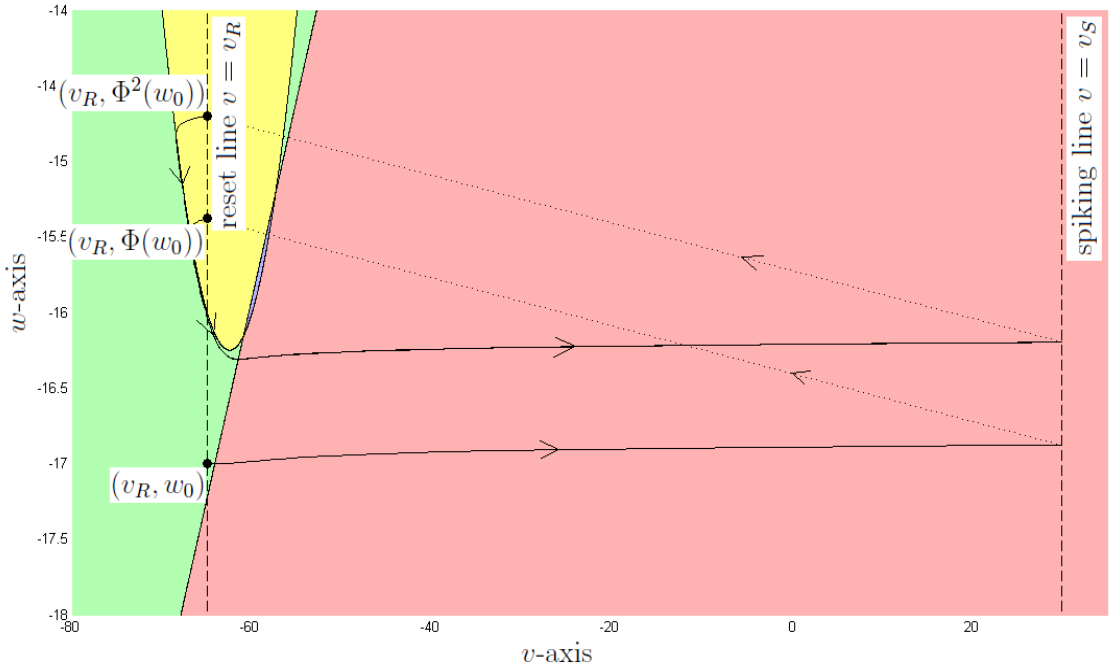

Figure 4.1: A solution of the model (4.1). Trajectory begins at (v_R, w_0) and evolves towards the right, reaching the spiking line and resetting to $(v_R, \Phi(w_0))$. The trajectory continues from this point, making a half-turn before going towards the spiking line, and then resetting to $(v_R, \Phi^2(w_0))$.

condition for trajectories to converge towards one another over time. The variational equation can also be used to assess convergence of trajectories. However, the orbits are invariant under reparametrization of the flow, therefore the convergence of orbits requires only the convergence of trajectories in any direction that is transverse to the flow. In other words, the stability of regular spiking depends only on the transverse convergence of trajectories. Our approach is to fix a transverse direction, onto which the variational equation is projected. The result is a quantity called the transverse local Lyapunov exponent (TLLE), which describes the rate of expansion of the transverse component of an initially transverse displacement. We express $\log|\Phi'|$ as the integral of the TLLE along trajectories, together with boundary terms that match the transverse direction to the reset and spiking lines. Using symmetry in the model equations, we estimate this integral and obtain sufficient conditions on the model parameters such that $\log|\Phi'| < 0$, i.e., such that Φ is non-expansive.

The TLLE is similar to the local Lyapunov exponent described in [5] and to the local divergence rate described in [7] and [18]; a comparison is made in Section 4.3. It is worth noting that the method described in Section 4.3 for obtaining the TLLE can be applied to any system determined by a twice continuously differentiable vector field and having a Poincaré map or a more general reset map of the type described here. For each choice of the transverse field an expression for the derivative of the map is obtained. A judicious choice of the transverse field may lead to a local exponent that has a convenient analytical or algebraic form, or that gives a more accurate measure of the separation of orbits than can be obtained using only the variational equation, as shown in Figure 4.2.

In Section 4.2 we summarize enough from [22] to give the reader a sense of the phase plane for the model. In Section 4.3 we derive the TLLE and express Φ' as the integral of the TLLE over trajectories of the model. In Section 4.4 this integral is estimated, and when the model has ≤ 1 critical point, sufficient conditions are given on the parameters of the model for Φ to be non-expansive (see Theorem 4.4.4) i.e., for regular spiking to be globally asymptotically stable. In Chapter 5 we consider three examples. In the first two examples the result follows directly from Theorem 4.4.4. In the third example, the model has two critical points. For this example we adapt the results of Section 4.4 and measure the separation/convergence of orbits in the phase plane in order to show that regular spiking is globally asymptotically stable.

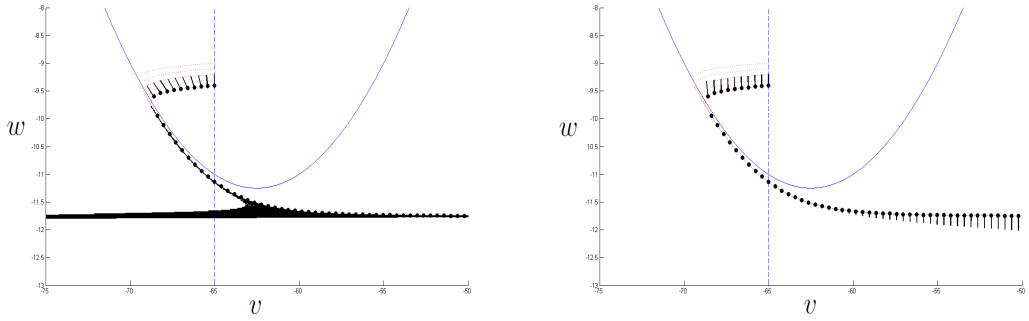

Figure 4.2: Evolution of displacement vectors along a trajectory. Displacement vectors portrayed as black lines. In (a), an initial displacement is placed in the vertical direction at the reset line, and then evolves according to the variational equation for the model. In (b), the same applies, except that the component of the displacement that is tangent to the flow has been discarded, and only the component of the displacement that is perpendicular to the flow is displayed. Removal of the component that is tangent to the flow gives a set of vectors that is much better behaved.

Note that the conditions given in Theorem 4.4.4 describe a relatively small region of parameter space. In [22] there are several results that describe the behaviour of Φ, including conditions for regular spiking, in terms of the values of Φ at certain points. The advantage of the present method is that it has a natural geometric interpretation in the phase plane, and conditions for regular spiking are given directly in terms of the model parameters.

The work by Touboul and Brette in [22] includes a detailed analysis of the AIF model. However, their analysis focuses primarily on the values assumed by the adaptation map. The present result is obtained by a more detailed analysis of the flow on the phase plane, and correspondingly leads to more direct conditions for regular spiking than those obtained in [22].

4.2 Phase Plane

In this section we describe the phase plane for the model; a more detailed discussion can be found in [22]. As mentioned in Section 4.1, we assume that the domain $\mathscr{D}$ of the adaptation map is all of $\mathbb{R}$.

Both the cases $v_S = \infty$ and $v_S < \infty$ are considered. As shown in Proposition 2.1 in [22], if $v_S = \infty$ it is important to note that F must satisfy

$$\lim_{v\to\infty} F(v)/v^{2+\epsilon} \geq \alpha > 0$$

for some $\epsilon > 0$ and some α in order to ensure that $w(t) < \infty$ as $t \to t_S^-$.

We now give some background on the phase plane for the model. Let $R = \{(v_R, w) : w \in \mathbb{R}\}$ denote the reset line. Let $X(v, w) = (f(v, w), g(v, w))^\top$ denote the vector field for the model, and for $x_0 \in \mathbb{R}^2$ and t such that the flow is defined, let $\phi(t, x_0)$ denote the flow of X, i.e., $\phi(0, x_0) = x_0$ and $\phi'(t, x_0) \equiv \partial_t\phi(t, x_0) = X(\phi(t, x_0))$. We are only interested in those solutions that start on the reset line, that is, $x_0 \in R$. By the assumption $\mathscr{D} = \mathbb{R}$, for each $x_0 \in R$ there is $w_S \in \mathbb{R}$ and $t_S > 0$ such that $\phi(t_S^-, x_0) = (v_S, w_S)$, which is understood as the limit as $t \to t_S^-$ when $v_S = \infty$.

On the (v, w) plane $v' = 0$ whenever $w = F(v) + I$, and $w' = 0$ whenever $w = bv$; these equations give the v-nullcline and w-nullcline respectively. Let w^* and w^{**} be the intersection of R with the v-nullcline and w-nullcline respectively, i.e., $w^* = F(v_R)+I$ and $w^{**} = bv_R$. Then,

1. $w^* > w^{**}$,
2. for $w_0 < w^*$ and $x_0 = (v_R, w_0)$, $\phi(t, x_0)$ moves to the right towards the spiking line, and
3. for $w_0 > w^*$, $\phi(t, x_0)$ makes a half-turn counter-clockwise around (v_R, w^*) before intersecting R below w^*.

The proof of these facts is contained in [22]; a brief argument is given below. Note that a critical point is a point where the vector field vanishes.

Critical points satisfy $F(v) - bv + I = 0$. By convexity of $F(v)$ and therefore of $F(v) - bv + I$, there are at most two critical points. If there are no critical points, by convexity of $F(v)$ the v-nullcline lies above the w-nullcline and $w^* > w^{**}$ (see Figure 4.3). Solutions with $w_0 < w^*$ are confined below the v-nullcline and move to the right, and solutions with $w_0 > w^*$ move initially to the left and down, intersect the v-nullcline moving straight down, and then move to the right, confined below the v-nullcline. When there is one critical point the nullclines intersect tangentially and the same is true. When there are two critical points denote them by $p_- = (v_-, w_-)$ and $p_+ = (v_+, w_+)$ with $v_- < v_+$. Note that the v-nullcline lies above the w-nullcline except when $v_- \leq v \leq v_+$ (see Figure 5.4 for an example). By convexity, $F'(v_-) < b$ and $F'(v_+) > b$. The Jacobian matrix

$$\begin{bmatrix} F'(v) & -1 \\ ab & -a \end{bmatrix}$$

has negative determinant at p_+, therefore p_+ is a saddle point. In Section 2.2 of [22] it is shown that the stable manifold Γ of the saddle point extends from p_+ down and towards the left at least to v_- below both nullclines; to see this, evolve the equations backwards in time. Since every initial condition on R leads to spiking, R and Γ are disjoint, therefore $v_R < v_-$, which implies that $w^* > w^{**}$ and that solutions with

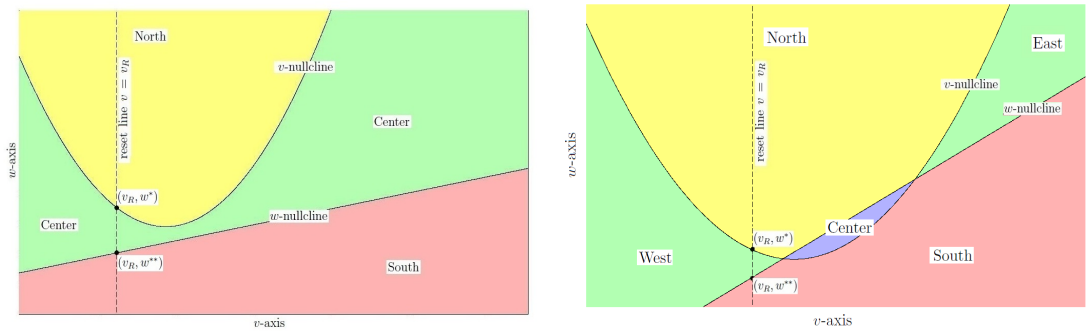

Figure 4.3: Phase plane for an example of model (4.1) with (a) no critical points and with (b) two critical points.

$w_0 > w^*$ make a half-turn. Since Γ is a continuous curve it is therefore confined to the half-plane $\{(v, w) : v > v_R\}$ and it must intersect the w-nullcline at some point (v, w) for which $v \leq v_-$, and this effectively prevents solutions with $w_0 < w^*$ from going above the w-nullcline, so that they have no choice but to move to the right towards the spiking line.

We can summarize the behaviour of solutions using the partition defined in Section 2.4 of [22]. If the model has ≤ 1 critical point let the *North*, *Center* and *South* regions be the sets that lie above, between, and below the nullclines respectively, as in Figure 4.3. If the model has two critical points, let the *North* region be the set $\{(w, v) : w \geq F(v) + I,\, w \geq bv\}$, the *Center* region be the set $\{(w, v) : F(v) + I < w < bv\}$ and the *South* region be the set $\{(w, v) : w \leq bv,\, w \leq F(v) + I\}$, and let the *West* and *East* regions be the left- and right-hand components respectively of the set $\{(w, v) : bv < w < F(v) + I\}$.

Then, if the model has ≤ 1 critical point, solutions that start on the reset line respect the order $North \to Center \to South$, i.e., no solution crosses from the South region into the North or Center regions, or from the Center region into the North region. If the model has two critical points, solutions that start on the reset line respect the order $North \to West \to South$. In the rest of this paper, we assume that solutions that start on the reset line intersect v_S in the South region; this holds trivially when $v_S = \infty$, and for most models used in practice this assumption holds.

4.3 Transverse Local Lyapunov Exponent

In this section we express $|\Phi'|$ as the integral of a tranverse local Lyapunov exponent (TLLE) along trajectories. The terminology TLLE is explained in greater detail at the bottom of Section 4.3.2. For now, we assume that $v_S < \infty$, and generalize to $v_S = \infty$ in Section 4.3.6. The symbol $|\cdot|$ is used to denote both the absolute value in $\mathbb{R}$ and the Euclidean norm $\sqrt{v^2 + w^2}$ of a vector $(v, w) \in \mathbb{R}^2$.

4.3.1 Expression for Φ' using the variational equation

First of all, Φ' is expressed in terms of the general solution to the variational equation (4.2) below. Let $S = \{(t, x_0) \in \mathbb{R}\times\mathbb{R}^2 : \phi(t, x_0) \text{ is well-defined}\}$ and define the matrix-valued function $T : S \to M_2(\mathbb{R})$ by $T(0, x_0) = I_2$ where I_2 is the 2×2 identity matrix, and such that

$$\frac{d}{dt}T(t, x_0) = DX(\phi(t, x_0))T(t, x_0) \tag{4.2}$$

It is a theorem (see Chapter 3, Theorem 3.5.4) that if X is continuously differentiable (which is the case here), then $T(t, x_0)$ is the derivative of $\phi(t, x_0)$ with respect to x_0, that is,

$$\phi(t, x_0 + \epsilon u) - \phi(t, x_0) = \epsilon T(t, x_0)u + o(\epsilon) \tag{4.3}$$

for $u \in \mathbb{R}^2$. Here $h(\epsilon) = o(\epsilon) \Leftrightarrow h(\epsilon)/\epsilon \to 0$ as $\epsilon \to 0$, where h denotes an arbitrary scalar- or vector-valued function. We would like to relate Φ' and T; the lemma that follows is useful for this task.

By assumption, all solutions with initial condition on the reset line $\{v = v_R\}$ reach the spiking line $\{v = v_S\}$ in finite time (see Definition 4.1.1 for details). Define $t_S : \mathbb{R} \to \mathbb{R}^+$ by $\phi(t_S(w_0), x_0) = \Phi(w_0) - d$, where $x_0 = (v_R, w_0)$ and $w_0 \in \mathbb{R}$. The following property of t_S is proved. Note that $^\top$ denotes the transpose, and for vectors $u, v \in \mathbb{R}^2$, both $u^\top v$ and $u \cdot v$ are used to denote the dot product of u and v. Let $e_1 = (1, 0)^\top$ and $e_2 = (0, 1)^\top$ denote the standard basis vectors.

Lemma 4.3.1. *The function $t_S(w_0)$ is differentiable.*

Proof. Fix $w_0 \in \mathbb{R}$ and let $x_0 = (v_R, w_0)$. Denote $t_S(w_0)$ simply by t_S. Define $H(\tau, \epsilon) = (\phi(t_S + \tau, x_0 + \epsilon e_2) - \phi(t_S, x_0)) \cdot e_1$. Then, $\partial_\tau H(0, 0) = X(\phi(t_s, x_0)) \cdot e_1$. The

assumption that solutions spike in the South region (which lies below the v-nullcline) guarantees that $X(\phi(t_S, x_0)) \cdot e_1 \neq 0$. The implicit function theorem then guarantees the existence of a unique function $\tau(\epsilon)$, at least continuously differentiable, defined for ϵ in an open set U containing 0, such that $H(\tau(\epsilon), \epsilon) = 0$, in other words, such that $\phi(t_S + \tau(\epsilon), x_0 + \epsilon e_2)$ lies on the spiking line $\{v = v_S\}$.

Now it is shown that $t_S(w_0 + \epsilon) = t_S(w_0) + \tau(\epsilon)$ for $\epsilon \in U$. Since τ is the unique continuous function on U such that $\tau(0) = 0$ and $\phi(t_S + \tau(\epsilon), x_0 + \epsilon e_2)$ lies on the spiking line, it is sufficient to show that $t_S(w_0 + \epsilon)$ is continuous for $\epsilon \in U$. Therefore suppose that $t_S(w_0 + \epsilon)$ fails to be continuous for some $\epsilon \in U$. Then there is a $\delta > 0$ and a sequence $(\epsilon_k) \to \epsilon$ such that $|t_S(\epsilon_k) - t_S(\epsilon)| \geq \delta$ for each $k \in \mathbb{N}$. There is a subsequence (ϵ_{k_n}) such that either $t_S(\epsilon_{k_n}) \geq t_S(\epsilon) + \delta$ for each n, or $t_S(\epsilon_{k_n}) \leq t_S(\epsilon) - \delta$ for each n. Applying the result of the last paragraph with $t_S(w_0)$ replaced by $t_S(w_0 + \epsilon)$ yields a contradiction in the first case, therefore suppose $t_S(\epsilon_{k_n}) \leq t_S(w_0 + \epsilon) - \delta$ for each n. The sequence $t_S(\epsilon_{k_n})$ is bounded, so it has a convergent subsequence with limit $t \leq t_S(w_0 + \epsilon) - \delta < t_S(w_0 + \epsilon)$. Since for each $k \in \mathbb{N}$, $\phi(t_S(\epsilon_k), x_0 + \epsilon_k e_2)$ lies on the spiking line, it follows by continuity that $\phi(t, x_0 + \epsilon e_2)$ lies on the spiking line, which is a contradiction. Therefore $t_S(w_0 + \epsilon) = t_S(w_0) + \tau(\epsilon)$ for $\epsilon \in U$.

□

The following expression relates Φ' and T. Note that the assumption that solutions spike in the South zone guarantees that $X^{\perp}(\phi(t_S, x_0)) \cdot e_2 \neq 0$.

Proposition 4.3.2. *Let T be defined as above, then for $x_0 = (v_R, w_0)$ and $w_0 \in \mathbb{R}$,*

$$\Phi'(w_0) = \frac{(X^{\perp}(\phi(t_S, x_0)))^{\top}}{X^{\perp}(\phi(t_S, x_0)) \cdot e_2} T(t_S, x_0) e_2$$

Proof. Fix $x_0 = (v_R, w_0)$ and write $(\Phi(w_0 + \epsilon) - \Phi(w_0))e_2 = \phi(t_S(w_0 + \epsilon), x_0 + \epsilon e_2) - \phi(t_S(w_0), x_0)$ in two parts as

$$(\phi(t_S(w_0 + \epsilon), x_0 + \epsilon e_2) - \phi(t_S(w_0), x_0 + \epsilon e_2)) + (\phi(t_S(w_0), x_0 + \epsilon e_2) - \phi(t_S, x_0))$$

Let $\Delta t_S(w_0; \epsilon)$ denote $t_S(w_0 + \epsilon) - t_S(w_0)$, then writing the Taylor expansion for ϕ with respect to the first argument, $\frac{d}{dt}\phi(t, x_0) = X(\phi(t, x_0))$ gives

$$\phi(t_S(w_0+\epsilon), x_0+\epsilon e_2) - \phi(t_S(w_0), x_0+\epsilon e_2)) = \Delta t_S(w_0; \epsilon) X(\phi(t_S(w_0), x_0+\epsilon e_2)) + o(\Delta t_S(w_0; \epsilon))$$

and (4.3) gives

$$\phi(t_S(w_0), x_0 + \epsilon) - \phi(t_S(w_0), x_0) = \epsilon T(t_S, x_0)e_2 + o(\epsilon)$$

By Lemma 4.3.1, t_S is differentiable, so that $\Delta t_S(w_0; \epsilon) = \epsilon t_S'(w_0) + o(\epsilon) = O(\epsilon)$ and

$$(\Phi(w_0 + \epsilon) - \Phi(w_0))e_2 = \epsilon t_S'(w_0)X(\phi(t_S(w_0), x_0 + \epsilon e_2) + \epsilon T(t_S, x_0)e_2 + o(\epsilon) \quad (4.4)$$

Take the dot product with $(X^\perp(\phi(t_S, x_0 + \epsilon e_2)))/(X^\perp(\phi(t_S, x_0 + \epsilon e_2)) \cdot e_2)$ on both sides, divide by ϵ and take $\epsilon \to 0$ in (4.4) to obtain

$$\Phi'(w_0) = \frac{(X^\perp(\phi(t_S, x_0)))^\top}{X^\perp(\phi(t_S, x_0)) \cdot e_2} T(t_S, x_0)e_2 \quad (4.5)$$

which proves Proposition 4.3.2. □

The expression for Φ' can be understood as "take a displacement in the e_2 direction at the reset line, evolve it along the trajectory, and then project onto the e_2 component of the (X, e_2) basis at the spiking line".

4.3.2 Expression for Φ' in terms of the TLLE

The above expression is helpful in relating Φ' to the flow. However, it contains the term $T(t, x_0)$, which is the solution to a two-dimensional nonautonomous linear system, and in order to estimate Φ' it would be nice to replace $T(t, x_0)$ with the solution of a one-dimensional linear differential equation. This is accomplished in the steps that follow by decomposing both the initial displacement e_2 and the evolution matrix $T(t, x_0)$ in terms of a basis that moves with the trajectory $\phi(t, x_0)$.

The following function, called the transverse local Lyapunov exponent (TLLE), appears in the result below:

$$L(x) \equiv \frac{X^\perp(x) \cdot [Y(x), X(x)]}{X^\perp(x) \cdot Y(x)} \quad (4.6)$$

Here $[Y, X] = DXY - DYX$ is the Jacobi bracket [8], also known as the commutator. The TLLE measures the rate of logarithmic expansion or contraction of a

small transversal as it evolves along a trajectory. The TLLE is similar to the local Lyapunov exponent (l.l.e.) described in [5]. However, the l.l.e. measures the rate of expansion with respect to the asymptotic expanding direction, whereas in this case the TLLE measures the rate of expansion with respect to a chosen transverse direction. The TLLE can be more accurately described as a transverse version of the local divergence rate described in [7] and [18]. The present terminology is chosen because Lyapunov exponent is a more familiar term and the TLLE is indeed a local exponent for transverse displacements.

The following result is proved.

Proposition 4.3.3. *Let* $C(x) \equiv \frac{X^{\perp}(x)\cdot Y(x)}{X^{\perp}(x)\cdot e_2}$ *and let* $L(x)$ *be defined as above. Then for* $w_0 \in \mathbb{R}$*,*

$$\log|\Phi'(w_0)| = \int_0^{t_S} L(\phi(s,x_0))ds + \log\left|\frac{C(\phi(t_S,x_0))}{C(x_0)}\right| \tag{4.7}$$

Proof. Differentiating $X(\phi(t,x_0)$ with respect to t gives

$$\frac{d}{dt}X(\phi(t,x_0)) = DX(\phi(t,x_0))X(\phi(t,x_0))$$

so that $X(\phi(t,x_0))$ solves (4.2), which implies that

$$X(\phi(t+\tau,x_0)) = T(t,\phi(\tau,x_0))X(\phi(\tau,x_0)) \tag{4.8}$$

for t, τ and x_0 such that the above expression is defined. This may be interpreted as "T leaves X invariant". Let Y be a vector field transverse to X, that is, $|X(x)\cdot Y(x)| < |X(x)||Y(x)|$ whenever $X(x) \neq 0$. Then if x is such that $X(x) \neq 0$, it follows that $X(x)$ and $Y(x)$ are linearly independent, and so the projectors $P_X(x)$ and $P_Y(x)$ given by

$$P_X(x) = \frac{X(x)(Y^{\perp}(x))^{\top}}{Y^{\perp}(x)\cdot X(x)} \quad \text{and} \quad P_Y(x) = \frac{Y(x)(X^{\perp}(x))^{\top}}{X^{\perp}(x)\cdot Y(x)}$$

are well-defined and satisfy $I_2 = P_X(x) + P_Y(x)$. Also,

$$T(t,x_0)P_X(x_0) = \frac{X(\phi(t,x_0))(Y^{\perp}(x_0))^{\top}}{Y^{\perp}(x_0)\cdot X(x_0)}$$

using (4.8). Write $T(t,x_0)$ as $T(t,x_0)I = T(t,x_0)P_X(x_0) + T(t,x_0)P_Y(x_0)$. Plugging into (4.5), observe that $(X^{\perp}(\phi(t_S,x_0)))^{\top}$ annihilates $X(\phi(t_S,x_0))$ in $T(t,x_0)P_X(x_0)$,

which leads to the expression

$$\Phi'(w_0) = \frac{(X^\perp(\phi(t_S, x_0)))^\top}{X^\perp(\phi(t_S, x_0)) \cdot e_2} T(t_S, x_0) Y(x_0) \frac{X^\perp(x_0) \cdot e_2}{X^\perp(x_0) \cdot Y(x_0)} \tag{4.9}$$

in which only the Y component of the initial displacement remains. Then, project $T(t_S, x_0)Y(x_0)$ onto the (X, Y) basis, i.e., let

$$\mu(t, x_0) = \frac{(Y^\perp(\phi(t, x_0)))^\top T(t, x_0) Y(x_0)}{Y^\perp(\phi(t, x_0)) \cdot X(\phi(t, x_0))}$$

be the magnitude of the X component and let

$$m(t, x_0) = \frac{(X^\perp(\phi(t, x_0)))^\top T(t, x_0) Y(x_0)}{X^\perp(\phi(t, x_0)) \cdot Y(\phi(t, x_0))}$$

be the magnitude of the Y component, so that $T(t, x_0)Y(x_0) = \mu(t, x_0)X(\phi(t, x_0)) + m(t, x_0)Y(\phi(t, x_0))$. Plugging this expression into (4.9), once again $(X^\perp(\phi(t_S, x_0)))^\top$ annihilates $X(\phi(t_S, x_0))$, which gives

$$\Phi'(w_0) = \frac{X^\perp(\phi(t_S, x_0)) \cdot Y(\phi(t_S, x_0))}{X^\perp(\phi(t_S, x_0)) \cdot e_2} m(t_S, x_0) \frac{X^\perp(x_0) \cdot e_2}{X^\perp(x_0) \cdot Y(x_0)} \tag{4.10}$$

This is a simpler expression than (4.5), since $m(t, x_0)$ satisfies the scalar differential equation (4.11) below. To derive this equation, note that $T(t, x_0)Y(x_0)$ solves (4.2), so that replacing $T(t, x_0)$ with $\mu(t, x_0)X(\phi(t, x_0)) + m(t, x_0)Y(\phi(t, x_0))$ in (4.2) gives

$$\frac{d\mu}{dt}X + \mu DXX + \frac{dm}{dt}Y + mDYX = (DX)(\mu X + mY)$$

Subtracting μDXX from both sides and taking the dot product with $X^\perp$ on both sides yields the equation

$$\frac{d}{dt}m(t, x_0) = L(\phi(t, x_0))m(t, x_0) \tag{4.11}$$

where $L(x)$, defined in (4.6), is the TLLE.

Observe that (4.11) is equivalent to the expression $\frac{d \log |m(t,x_0)|}{dt} = L(\phi(t, x_0))$. Taking the logarithm of the absolute value in (4.10), and using (4.11) and the fundamental

theorem of calculus gives

$$\log|\Phi'(w_0)| = \int_0^{t_S} L(\phi(s,x_0))ds + \log\left|\frac{C(\phi(t_S,x_0))}{C(x_0)}\right| \tag{4.12}$$

where $C(x) \equiv \frac{X^\perp(x)\cdot Y(x)}{X^\perp(x)\cdot e_2}$ is a boundary condition. The integral can be understood as the net factor of expansion of a transversal, summed over a trajectory from the reset line to the spiking line.

□

Remark 1. *It follows from Proposition 4.3.3 that Φ is non-expansive whenever*

$$\int_0^{t_S} L(\phi(s,x_0))ds + \log\left|\frac{C(\phi(t_S,x_0))}{C(x_0)}\right| < 0 \tag{4.13}$$

We see that the above inequality is a condition for regular spiking that only requires estimating the integral of the function L along the flow ϕ, between the reset and spiking lines.

4.3.3 Choice of transverse fields

In the expression (4.13) the transverse field Y is still left unchosen. To estimate Φ', two choices of the transverse field are used. It turns out to be useful first to rescale X to unit vectors, in which case the integral in (4.13) is a path integral. Let $\hat{X}(x) \equiv X(x)/|X(x)|$ when $X(x) \neq 0$ and $\hat{X}(x) \equiv 0$ when $X(x) = 0$. The choice $Y = e_2 \equiv (0,1)^\top$ is called the *vertical* field, and the choice $Y = \hat{X}^\perp$ is called the *orthogonal* field. These fields are chosen because trajectories either go straight to the right towards the spiking line, in which $Y = e_2$ is convenient, or else trajectories make a half-turn before going towards the spiking line, in which case it is necessary to have Y turn with the trajectories, and $Y = \hat{X}^\perp$ is then the simplest choice. Note that

$$D\hat{X} = (I_2 - \hat{X}\hat{X}^\top)\frac{DX}{|X|}$$

when $X \neq 0$, where I_2 is the 2×2 identity matrix. For $Y = e_2$, $DY = 0$ and so

$$L_V = \frac{\hat{X}^\perp \cdot \left(\frac{DX}{|X|}e_2\right)}{\hat{X}^\perp \cdot e_2}$$

is the exponent for the vertical field. Using

$$DX = \begin{bmatrix} f_v & f_w \\ g_v & g_w \end{bmatrix} \tag{4.14}$$

and $\hat{X}^{\perp} = (-g, f)^{\top}/(f^2 + g^2)^{1/2}$ gives

$$L_V = \frac{g_w f - f_w g}{f^2(1 + (g/f)^2)^{1/2}} \tag{4.15}$$

Similar computations give the exponent

$$L_O = \frac{g^2 f_v - fg(f_w + g_v) + f^2 g_w}{(f^2 + g^2)^{3/2}} \tag{4.16}$$

for the orthogonal field.

We distinguish the cases $w_0 < w^*$ and $w_0 > w^*$, using the results of Section 2. Recall that (v_R, w^*) is the unique point of intersection of the reset line with the v-nullcline. Since $\hat{X}$ is used to estimate Φ', let $\phi(r, x_0)$ denote the flow for $\hat{X}$ rather than X. The r is used to emphasize that the independent variable is now the arc length parameter and not time.

4.3.4 Case $w_0 < w^*$

If $w_0 < w^*$ then for $x_0 = (v_R, w_0)$, $\phi(r, x_0)$ moves to the right, in which case the vertical field is a natural choice. Notice that the boundary condition $C_V(x)$ for the vertical field is identically equal to 1. Let r_S be such that $\phi(r_S, x_0)$ is on the spiking line. This gives

$$\log |\Phi'(w_0)| = \int_0^{r_S} L_V(\phi(s, x_0))ds \tag{4.17}$$

and the sufficient condition

$$\int_0^{r_S} L_V(\phi(s, x_0))ds < 0 \tag{4.18}$$

for Φ to be non-expansive on $(-\infty, w^*)$.

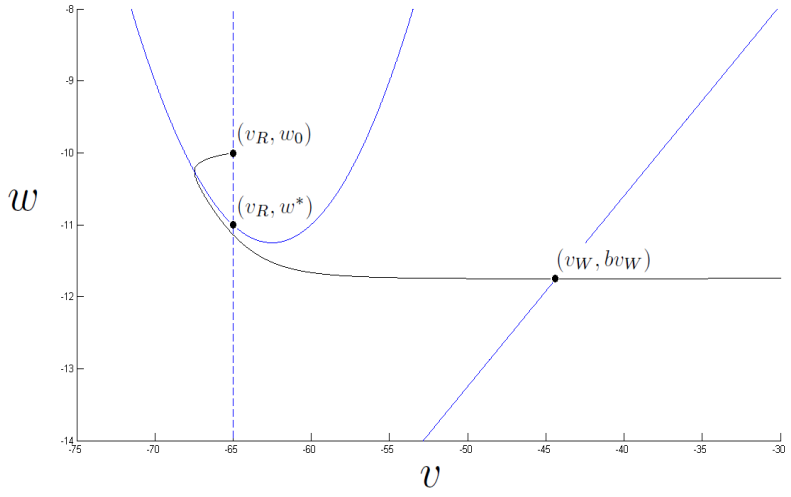

Figure 4.4: Depiction of a trajectory with $w_0 > w^*$

4.3.5 Case $w_0 > w^*$

If $w_0 > w^*$ then for $x_0 = (v_R, w_0)$ it follows from the discussion in Section 2 that $\phi(r, x_0)$ has a unique point of intersection $p_W = (v_W, bv_W) = \phi(r_W, x_0)$ with the w-nullcline and moves to the right at least from p_W up to the spiking line, as shown in Figure 4.4. The orthogonal field is used from the reset line up to p_W and the vertical field is used from p_W up to the spiking line; since $w' = 0$ on the w-nullcline, $\hat{X}^{\perp}(p_W)$ and e_2 are parallel, i.e., the two fields line up at p_W. This gives

$$\log|\Phi'(w_0)| = \int_0^{r_W} L_O(\phi(s, x_0))ds + \int_{r_W}^{r_S} L_V(\phi(s, x_0))ds + \log\left|\frac{C_V(\phi(r_S, x_0))}{C_O(x_0)}\right| \quad (4.19)$$

Note that $C_V \equiv 1$ and that $|C_O(x)| \geq 1$ for each x, so that $\log\left|\frac{C_V(\phi(r_S,x_0))}{C_O(x_0)}\right| \leq 0$. This gives the sufficient condition

$$\int_0^{r_W} L_O(\phi(s, x_0))ds + \int_{r_W}^{r_S} L_V(\phi(s, x_0))ds < 0 \quad (4.20)$$

for Φ to be non-expansive on (w^*, ∞). Abusing terminology somewhat, we refer to the integrals in (4.18) and to (4.20) as *contraction integrals*.

4.3.6 Extension to $v_S = \infty$

In [22] it is shown that if $F(v)/v^{1+\epsilon} \geq \alpha > 0$ for some α and some $\epsilon > 0$ as $v \to \infty$, and if a solution $(v(t), w(t))$ has $\lim_{t \to t_S^-} v(t) = \infty$, then $\lim_{t \to t_S^-} w(t)$ exists and is finite. In this case, when $v_S = \infty$ the adaptation map $\Phi(w_0)$ is given by the pointwise limit of $\Phi(w_0)$ for finite v_S, as $v_S \to \infty$. Here we show that the expressions in (4.17) and in (4.19) are valid when $v_S = \infty$. We begin with the following proposition.

Proposition 4.3.4. *Let J be a closed and bounded interval contained in either $\{w > w^*\}$ or $\{w < w^*\}$. Then $\Phi(w_0)$, which depends on v_S, converges uniformly for $w_0 \in J$ as $v_S \to \infty$.*

Proof. The proof is similar to the proof of Theorem 2.1 in [22]. Observe first of all that there is a lower-bound trajectory, i.e., a trajectory which as $v \to \infty$ has w-value less than that of any other trajectory, for fixed v. Using the results of Section 4.2, if $J \subset \{w < w^*\}$ the lower-bound trajectory is the one with the smallest initial value of w_0, and if $J \subset \{w > w^*\}$ it is the trajectory with the largest initial value of w_0. Let v_1 be such that all trajectories lie in the South region for $v > v_1$. An example of such a value is $\frac{1}{b} \sup J$, the intersection of the line $\{w = \sup J\}$ with the w-nullcline, using the fact that J is bounded above, $w' < 0$ above the w-nullcline, and solutions starting on the reset line remain below the w-nullcline after crossing it, as proved in Section 4.2. Let (v_1, w_1) be a point on the lower-bound trajectory. Then for $v > v_1$, each solution $(v(t), w(t))$ satisfies the estimate

$$\frac{dw(t)}{dv(t)} \leq \frac{a(bv(t) - w_1)}{F(v(t)) - bv(t) + I}$$

using the fact that $w(t)$ is increasing in the South region and $w < bv$ in the South region. If t_S denotes the spiking time of a trajectory and $w_S = \lim_{t \to t_S^-} w(t)$ for that trajectory, then for t sufficiently close to t_S, it follows that

$$w_S - w(t) \leq \int_{v(t)}^{\infty} \frac{a(bv - w_1)}{F(v) - bv + I}$$

and the right-hand side vanishes as $v(t) \to \infty$ whenever $F(v)$ satisfies the constraint mentioned at the beginning of Section 4.2. Since the right-hand side of the above equation is independent of the particular trajectory considered, it follows that convergence is uniform with respect to w_0. □

A similar fact is now proved for $\log|\Phi'(w_0)|$.

Proposition 4.3.5. *Let J be a closed and bounded interval contained in either $\{w > w^*\}$ or $\{w < w^*\}$. Then $\log|\Phi'(w_0)|$ converges uniformly for $w_0 \in J$ as $v_S \to \infty$.*

Proof. We prove the stronger statement, that the expressions given in (4.17) and (4.19) converge uniformly for $w_0 \in \{w < w^*\}$ and $w_0 \in \{w > w^*\}$. The boundary condition C_O appearing in (4.19) converges uniformly since $\hat{X}^\perp \cdot e_2$ approaches 1 uniformly in w on the set $\{(v, w) : w < bv\}$, as $v \to \infty$. Therefore it is enough to show that

$$\int_0^{r_S} L_V(\phi(s, x_0))ds \tag{4.21}$$

converges uniformly for x_0 in the South region as $r_S \to \infty$, since this implies the uniform convergence for $w_0 \in \{w < w^*\}$ of the integral in (4.17) and for $w_0 \in \{w > w^*\}$ of the second integral in (4.19). Using v as the integration variable, $L_V = (g - af)/(f^2(1 + (g/f)^2)^{1/2})$ and $ds = (1 + (g/f)^2)^{1/2}dv$, so that the above integral becomes

$$\int_0^{v_S} \frac{g/f - a}{f} dv$$

where g and f are integrated along the trajectory. For $v > v_+$, $F(v) + I > bv$ since the v-nullcline lies above the w-nullcline, and so $af = a(F(v) - w + I) > a(bv - w) = g$. Since f and g are positive below the w-nullcline, $0 < g/f < a$. Using the constraint on $F(v)$ mentioned at the beginning of Section 2, and using $w < bv$, $f/v^{2+\epsilon} \geq (F(v) - bv + I)/v^{2+\epsilon} \geq \alpha > 0$ for v large enough. Therefore the quantity

$$\int_{v_S}^{\infty} \frac{a}{\alpha v^{2+\epsilon}} dv = \frac{a}{\alpha(1+\epsilon)v_S^{1+\epsilon}}$$

vanishes as $v \to \infty$, and this implies the uniform convergence, for x_0 in the South region, of (4.21) as $r_S \to \infty$. □

The above two propositions are combined to produce the following result.

Proposition 4.3.6. *The function $\Phi(w_0)$ is differentiable in the case $v_S = \infty$, and $\log|\Phi'(w_0)|$ is given by the limit as $r_S \to \infty$ of the expression in (4.17) when $w_0 < w^*$, and by the limit as $r_S \to \infty$ of the expression in (4.19) when $w_0 > w^*$.*

Proof. Let (v_n) be any sequence of values of v_S such that $v_n \to \infty$, then corresponding sequences (Φ_n) and (Φ'_n) are obtained by letting $v_S = v_n$ for each n. It is a fact from calculus that on a common interval of definition J, if the sequences (Φ_n) and (Φ'_n) converge uniformly on J, then $\lim_{n\to\infty} \Phi_n = \Phi$ is differentiable and $\Phi' = \lim_{n\to\infty} \Phi'_n$ on J. According to Propositions 4.3.4 and 4.3.5, if J is a closed and bounded interval contained in either $\{w > w^*\}$ or $\{w < w^*\}$, then both $\Phi(w_0)$ and $\log|\Phi'(w_0)|$ converge uniformly for $w_0 \in J$ as $v_S \to \infty$. Thus, for $w_0 \neq w^*$ let J be as above such that $w_0 \in J$. From the continuity of $\log|\cdot|$, it follows that the sequences (Φ_n) and (Φ'_n) converge uniformly on J. The statement of the proposition then follows at w_0, using again the continuity of log and the fact that $r_S \to \infty$ as $v_S \to \infty$, since r_S is an arc length parameter. Since $w_0 \neq w^*$ is arbitrary, the result follows. □

The results of Section 4.3 are summarized in the following theorem.

Theorem 4.3.7. *Let $\mathscr{D}$ denote the domain of Φ (see Definition 4.1.1). Then, if $\mathscr{D} = \mathbb{R}$, Φ is non-expansive on $\mathbb{R}$ when* (4.18) *is satisfied for all $w_0 < w^*$ and* (4.20) *is satisfied for all $w_0 > w^*$. If $v_S = \infty$ the integrals in* (4.18) *and* (4.20) *with upper endpoint r_S are improper integrals.*

The above theorem gives a sufficient but not a necessary condition for Φ to be non-expansive. As discussed in the introduction, if Φ is non-expansive and its domain is the whole real line then regular spiking is globally asymptotically stable.

4.4 Estimation of the integral

In this section we show that (4.18) is satisfied when the model has ≤ 1 critical point, and give sufficient conditions for (4.20), without assumptions on the critical points. In the case of ≤ 1 critical point, Theorem 4.4.4 gives sufficient conditions on the model parameters for Φ to be non-expansive.

Note that $L_V(x)$ is undefined on the v-nullcline. For a trajectory $\phi(r, x_0)$ defined for r in an interval U and disjoint from the v-nullcline, as in the previous section we let v be the integration variable, so that the integral of L_V over the trajectory is

$$\int_U \frac{g - af}{f^2} dv$$

The integrand is understood to be a function of $\phi(r, x_0)$ where r is a function of the integration variable; the argument to the integrand is often dropped in this section for efficiency of notation. When the model has ≤ 1 critical point, off the v-nullcline $L_V(x) < 0$ almost everywhere. This is because in this case the w-nullcline lies below the v-nullcline except maybe at a single point, i.e., $bv < F(v) + I$ almost everywhere, so that $g = a(bv - w) < a(F(v) - w + I) = af$, or $g - af < 0$ almost everywhere. Therefore the following is true.

Proposition 4.4.1. *If the model has ≤ 1 critical point, then the condition in* (4.18) *is satisfied, and the second term in* (4.20) *is negative.*

Thus, if the model has ≤ 1 critical point, then for Φ to be non-expansive it is sufficent to have

$$\int_0^{r_W} L_O(\phi(s, x_0))ds < 0 \tag{4.22}$$

for $\phi(r, x_0)$ as described in Section 4.3.5. When the nullclines cross, i.e., when there are two critical points, L_V is positive on the strip $\{(v, w) : v_- < v < v_+\}$, which indicates separation of the orbits on that strip; this fact is addressed in the example in Section 5.3.

In the rest of this section we focus on the integral in (4.22). This is the integral of L_O over trajectories whose initial point lies on the reset line above w^* and whose terminal point lies on the w-nullcline. Except in the statement of Theorem 4.4.4, in the rest of this section nothing is assumed about the critical points.

To estimate the integral, trajectories are split into two pieces and the integrand is split into three pieces. Given $\phi(r, x_0)$, let $(v_V, F(v_V)) = \phi(r_V, x_0)$ be its unique point of intersection with the v-nullcline. Then for $0 \leq r \leq r_V$, $\phi(r, x_0)$ is contained in the subset

$$A = \{(v, w) : v \leq v_R, w \geq F(v) + I\}$$

of the North region. Let v_T be the unique value of v such that $F'(v) = 0$, and let $w_T = F(v_T)$. Let $v_{max} = \max\{v_R, v_T\}$, and define the subset $B = \{(v, w) : bv \leq w \leq l(v)\}$ of the Center/West region, where

$$l(v) = \{(v, w) : w = F(v) + I, v \leq v_{max}\} \cup \{(v, w) : w = F(v_{max}) + I, v \geq v_{max}\}$$

is the line that coincides with the v-nullcline to the left of v_{max} and extends horizon-

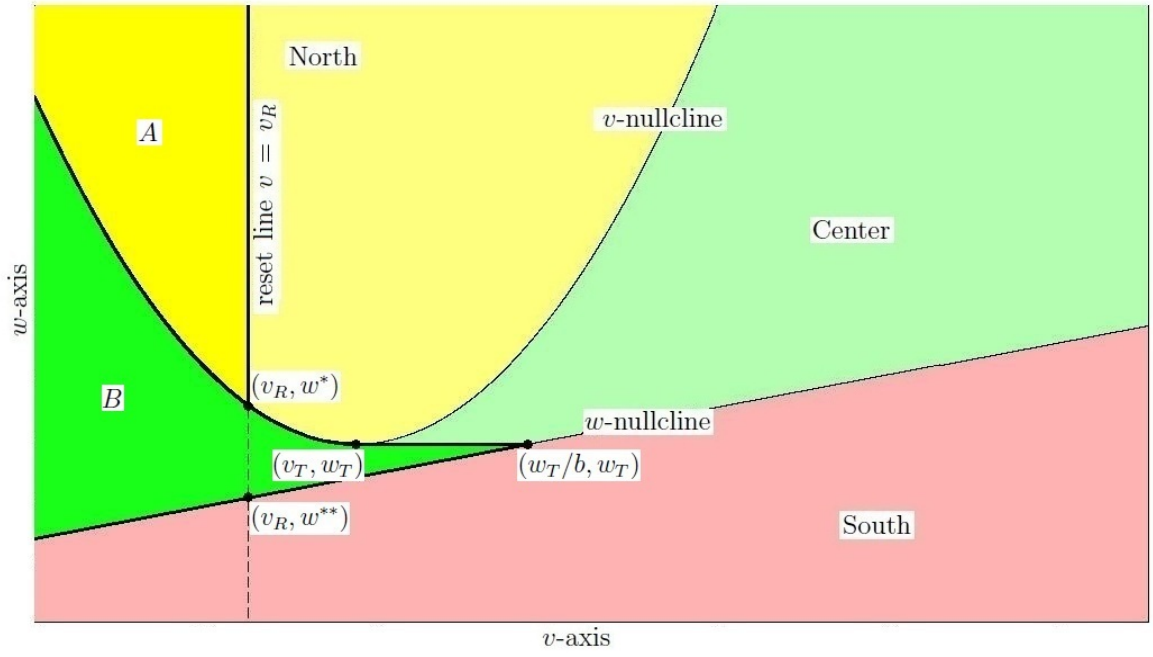

Figure 4.5: Phase plane for an example of model (4.1), with sets A and B bounded by the solid curves.

tally to the right of v_{max}; see Figure 4.5. Then, for $r_V \leq r \leq r_W$, $\phi(r, x_0)$ is contained in B. We split L_O into three parts:

$$L_O = G + H + J \tag{4.23}$$

where

$$G = \frac{g^2 F'}{(f^2+g^2)^{3/2}}, \quad H = \frac{(1-ab)fg}{(f^2+g^2)^{3/2}}, \quad J = \frac{-f^2 a}{(f^2+g^2)^{3/2}} \tag{4.24}$$

after substituting values in (4.16) for the partial derivatives of f and g according to (4.1). Now, J is everywhere negative, but G is positive when $F' > 0$, i.e., when $v > v_T$, and if $ab < 1$, which is assumed later, then H is non-negative when f and g have the same sign. Therefore we estimate the integrals of H and G.

4.4.1 Estimation of H

We give sufficient conditions for the integral of H along trajectories in the set $A \cup B$, i.e.,

$$\int_0^{rw} \frac{(1-ab)fg}{(f^2+g^2)^{3/2}} ds \tag{4.25}$$

to be negative. The integral is taken along the first half of trajectories described in Section 4.3.5. Since s is the integration variable, trajectories are written $\phi(s, x_0)$.

Proposition 4.4.2. *Suppose that $ab < 1$, $F'(v_R) < -a$ and $F'(v_R)+F'(w_T/b) < -2a$, where $w_T = F(v_T)$, and v_T is the unique value of v for which $F'(v) = 0$. Then the integral in (4.25) is negative.*

Proof. Let $z = f/g$, then z is well-defined on $A \cup B$ since $g \neq 0$ off the w-nullcline. First we show that $dz/ds \neq 0$, and then use z as the integration variable. Now

$$\frac{dz(\phi(s,x_0))}{ds} = \nabla z \cdot \frac{d\phi(s,x_0)}{ds}$$

Since s is the arc length parameter, $d\phi(s,x_0)/ds = (f^2+g^2)^{-1/2}(f,g)^\top$. Thus,

$$\begin{aligned}
\frac{dz}{ds} &= (f^2+g^2)^{-1/2}\big[f\partial_v z + g\partial_w z\big] \\
&= (f^2+g^2)^{-1/2}\big[f\frac{f_v g - f g_v}{g^2} + g\frac{f_w g - f g_w}{g^2}\big] \\
&= (f^2+g^2)^{-1/2}\big[-g_v(f/g)^2 + (f_v - g_w)(f/g) + f_w\big] \\
&= (f^2+g^2)^{-1/2}\big[-abz^2 + (F'+a)z - 1\big]
\end{aligned} \tag{4.26}$$

On A, $f \leq 0$ and $g < 0$ and so $z \geq 0$. Since $F'(v_R) < -a$ by assumption, $F'' > 0$ by convexity and $v < v_R$ on A it follows that $F' < -a$ on A. From this and from (4.26) it follows that $dz/ds < 0$ on A. In other words, trajectories starting on the reset line above w^* curve to the left between the reset line and the v-nullcline. Observe that $z < 0$ on B since $f > 0$ and $g < 0$ on B. If $dz/ds = 0$ at a point on B then

$$\frac{d}{ds}((f^2+g^2)^{1/2}\frac{dz}{ds}) = (-2abz + (F'+a))\frac{dz}{ds} + F''z = F''z < 0$$

since $F'' > 0$ and $z < 0$ on B. Also, $dz/ds = 0$ implies

$$\frac{d}{ds}((f^2+g^2)^{1/2}\frac{dz}{ds}) = (f^2+g^2)^{1/2}\frac{d^2z}{ds^2}$$

Therefore $dz/ds = 0 \Rightarrow d^2z/ds^2 < 0$ on B. In other words, if $\phi(s', x_0) \in B$ and $dz(\phi(s', x_0))/ds < 0$ then $dz(\phi(s, x_0))/ds < 0$ for all s such that $\phi(s'', x_0) \in B$ for $s' \leq s'' \leq s$. Now, $dz/ds < 0$ on the v-nullcline. Therefore, any trajectory that enters B by crossing the v-nullcline has $dz/ds < 0$ so long as it remains in B. This includes trajectories $\phi(s, x_0)$ with $x_0 = (v_R, w_0)$ and $w_0 > w^*$, for $r_V \leq s \leq r_W$. Thus, (4.25) can be re-written with z as the integration variable. Using (4.26) and the definition of z, (4.25) becomes

$$-\int_{z_2}^{z_1} \frac{1}{|g|} \frac{(1-ab)z}{(1+z^2)^{3/2}} \frac{ds}{dz} dz = \int_{z_2}^{z_1} \frac{(1-ab)z}{(1+z^2)} (abz^2 - (F'+a)z + 1)^{-1} dz \equiv \int_{z_2}^{z_1} Z(z) dz$$

In order for the above integral to be negative, it is sufficient that

1. $Z(z) < 0$ for $z_2 \leq z < 0$ and $Z(z) > 0$ for $0 < z \leq z_1$,
2. $[-z_1, z_1]$ lies in the domain of integration, and
3. $|Z(-z)| > |Z(z)|$ for $0 < z \leq z_1$.

Since $z = f/g \to -\infty$ as ϕ approaches the w-nullcline, Point 2 holds. Also, $ab < 1$ by assumption and $dz/ds < 0$ on $A \cup B$, thus Point 1 holds. It can be checked by comparison that $F'(v(z)) + F'(v(-z)) < -2a$, for $0 < z \leq z_1$, is sufficient for Point 3 to hold. Since $z > 0$ on A and $z < 0$ on B, and since $F'' > 0$, this last expression is true whenever $F'(v_R) + F'(w_T/b) < -2a$. This is because v_R and w_T/b are the largest v values on A and B respectively. □

4.4.2 Estimation of G

We estimate the integral of G along trajectories on $A \cup B$. Let $F'(v_R) < 0$, then G is negative on A, therefore we focus on the integral of G along trajectories on B, which is given by

$$\int_{r_V}^{r_W} \frac{g^2 F'}{(f^2+g^2)^{3/2}} ds \tag{4.27}$$

Since s is the integration variable, trajectories are written $\phi(s, x_0)$. The integral is taken along trajectories with $x_0 = (v_R, w_0)$ where $w_0 > w^*$, $\phi(r_W, x_0) = (v_W, bv_W)$, as in Section 4.3.5, and $\phi(r_V, x_0) = (v_V, F(v_V))$ for some v_V, i.e., $\phi(r_V, x_0)$ lies on the v-nullcline.

Proposition 4.4.3. *Suppose that $F'(v_R) < 0$. Let v_T denote the unique v such that $F'(v) = 0$, and let $w_T = F(v_T)$. Then the integral in (4.27) is negative when $F(v_R) \geq F(w_T/b)$.*

Proof. To estimate the integral in (4.27) we use the value of $F(v)$ on path segments as the integration variable. Note that the function $F(v)$ is two-to-one and with the exception of $F(v_T)$, each point in its range has one preimage to the left of v_T, and one preimage to the right of v_T. Let x_0 be fixed and ignore the point $\phi(r_V, x_0)$, then $\phi(s, x_0)$ lies below the v-nullcline and so it has $v' > 0$ and admits the parametrization $\phi(v)$. Letting $\phi_- = \operatorname{Ran}\phi(v) \cap \{(v, w) : v < v_T\}$ and $\phi_+ = \operatorname{Ran}\phi(v) \cap \{(v, w) : v > v_T\}$, then ϕ_- and ϕ_+ admit the parametrizations $\phi_-(y)$ and $\phi_+(y)$, where $y = F(v)$. Note that $ds/dy = (ds/dv)(dv/dy)$ and that

$$\frac{ds}{dv} = \frac{(f^2 + g^2)^{1/2}}{f} = (1 + (g/f)^2)^{1/2} \tag{4.28}$$

blows up only on the v-nullcline and

$$\frac{dv}{dy} = \frac{1}{F'} \tag{4.29}$$

blows up only when $v = v_T$, and both functions are non-zero. We can then write the integral in (4.27), with improper integrals implied at $F(v_V)$ and $F(v_T)$), as

$$-\int_{F(v_T)}^{F(v_V)} \frac{g_-^2 F_-'}{(f_-^2 + g_-^2)^{3/2}} \frac{ds_-}{dy} dy + \int_{F(v_T)}^{F(v_W)} \frac{g_+^2 F_+'}{(f_+^2 + g_+^2)^{3/2}} \frac{ds_+}{dy} dy$$

where $f_\pm = f(\phi_\pm(y))$ and similarly for the other functions. Let $x = (g/f)^2$. Using (4.28) and (4.29), this simplifies to

$$-\int_{F(v_T)}^{F(v_V)} \frac{x_-}{|f_-|(1 + x_-)} dy + \int_{F(v_T)}^{F(v_W)} \frac{x_+}{|f_+|(1 + x_+)} dy = -\int_{F(v_T)}^{F(v_4)} V_-(y) dy + \int_{F(v_T)}^{F(v_W)} V_+(y) dy$$

where the last equalities define $V_-(y)$ and $V_+(y)$. In order to show this integral is negative it is sufficient to show that

1. $F(v_V) - F(v_T) \geq F(v_W) - F(v_T)$ and that
2. $V_-(y) > V_+(y)$ for $F(v_T) < y \leq F(v_W)$

Since $F(v_V) > F(v_R)$ and $F(w_T/b) > F(v_W)$ for all path segments, for Point 1 to

hold it is sufficient that $F(v_R) \geq F(w_T/b)$. To verify Point 2, it is sufficient to have $f_-(y) < f_+(y)$ and $x_-(y) > x_+(y)$, since $d(x/(1+x))/dx > 0$. Note that if $\phi(v) = (v, w(v))$, then $dw(v)/dv = g/f < 0$ on B. Therefore, $w_-(y) > w_+(y)$, so that

$$f_-(y) = y - w_-(y) + I < y - w_+(y) + I = f_+(y)$$

Then, since $b > 0$ and $dw/dv < 0$,

$$dg(\phi(v))/dv = a(b - dw(v)/dv) > 0$$

and since g is negative, this gives

$$|g_-(y)| > |g_+(y)|$$

so that $x_-(y) > x_+(y)$, and the proposition is proved. □

Remark 2. *Note that if F is symmetric about v_T, then the condition in Proposition 4.4.3 reduces to $v_R + w_T/b \leq 2v_T$. In particular, this is the case when $F(v) = v^2$.*

We summarize the main result of this section.

Theorem 4.4.4. *Suppose the model has ≤ 1 critical point. Let v_T be the unique v for which $F'(v) = 0$, and let $w_T = F(v_T)$. Suppose that $ab < 1$, $F'(v_R) < -a$, $F'(v_R) + F'(w_T/b) < -2a$ and $F(v_R) \geq F(w_T/b)$. Then all orbits under Φ converge to a unique fixed point.*

Proof. If there is at most one critical point then by Proposition 4.4.1, the condition in (4.18) is satisfied, which implies that $|\Phi'| < 1$ on $(-\infty, w^*)$. Together, Propositions 4.4.1, 4.4.2 and 4.4.3 imply (4.20), so that $|\Phi'| < 1$ on (w^*, ∞). Since $|\Phi'| < 1$ almost everywhere, Φ is non-expansive, and so its fixed point is unique and globally attracting. □

The above is a sufficient condition on the model parameters for all initial conditions on the reset line to converge to a regular spiking behaviour, when the model has at most one critical point. In the next section we give three examples. The first two examples satisfy the conditions of Theorem 4.4.4. In the third example the model has two critical points and we need to account for expansion on the strip $\{(v, w) : v_- < v < v_+\}$.

Chapter 5

Examples

In this chapter we present three examples, one each of the quartic model $F(v) = v^4 + 2av$ [20], the exponential model $F(v) = e^v - v$ [2] and the Izhikevich model $F(v) = 0.04v^2 + 5v + 140$ [11], and in each case it is proved that regular spiking occurs. In the first two examples, parameter values are chosen so that Theorem 4.4.4 applies, from which regular spiking follows. In the third example the vector field has two critical points, and some additional work is required.

5.1 Quartic Model

Take the model (4.1) and let $F(v) = v^4 + 2av$, for the same a as in the equation for w' in the model (4.1). This is the quartic model described by Touboul in [20]. Taking the parameter values $a = 0.2, b = 2$, $I = 1$ and $v_R = -1$ gives the phase plane shown in Figure 5.1(a). Parameter values are chosen to illustrate the application of Theorem 4.4.4.

In this example the vector field has no critical points. Taking $d = 1.5$ and $v_S = \infty$ gives the adaptation map $\Phi(w_0)$ shown in Figure 5.2(a) (Φ is computed numerically). Observe that $|\Phi'(w_0)| < 1$ in the region shown, so that Φ is contracting in this region. Taking the initial condition $w_0 = -5$ on the reset line gives the solution shown in Figure 5.2(b), which appears to converge to a regular spiking pattern. To check that all initial conditions converge to regular spiking, it suffices to verify the conditions of Theorem 4.4.4. We readily compute that $ab = 0.4 < 1$, and that $F'(v_R) = 4(-1)^3 + 2(0.2) = -3.6 < -0.2 = -a$. Here v_T is given by $4v_T^3 + 2a = 0$ or $v_T = (-a/2)^{1/3} = (-0.1)^{1/3} \approx 0.46$, and $w_T = v_T^4 + 2av_T \approx 0.23$. $F'(w_T/b) \approx 0.41$ so

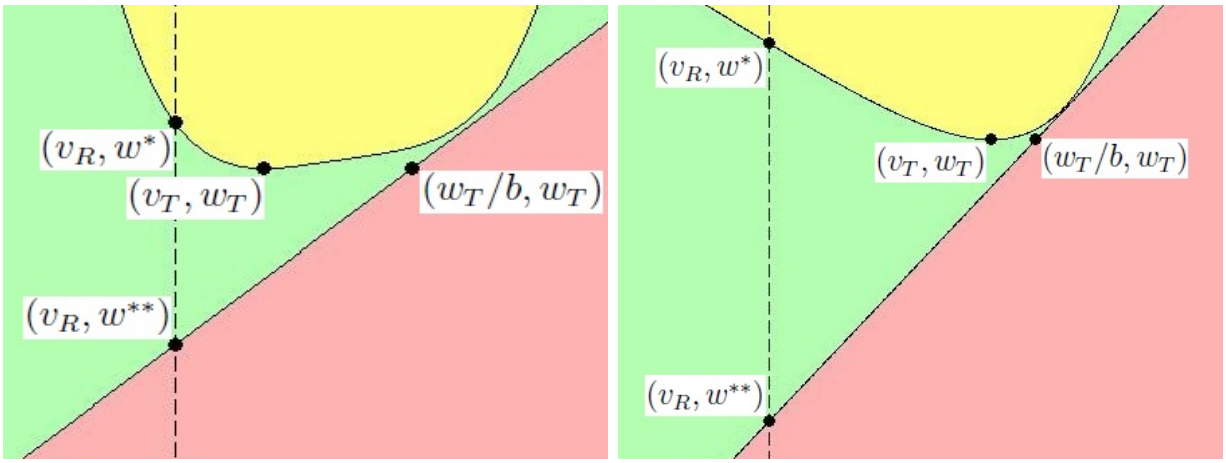

(a) Quartic model (b) Exponential model

Figure 5.1: Phase plane for the first two examples, neither of which have critical points

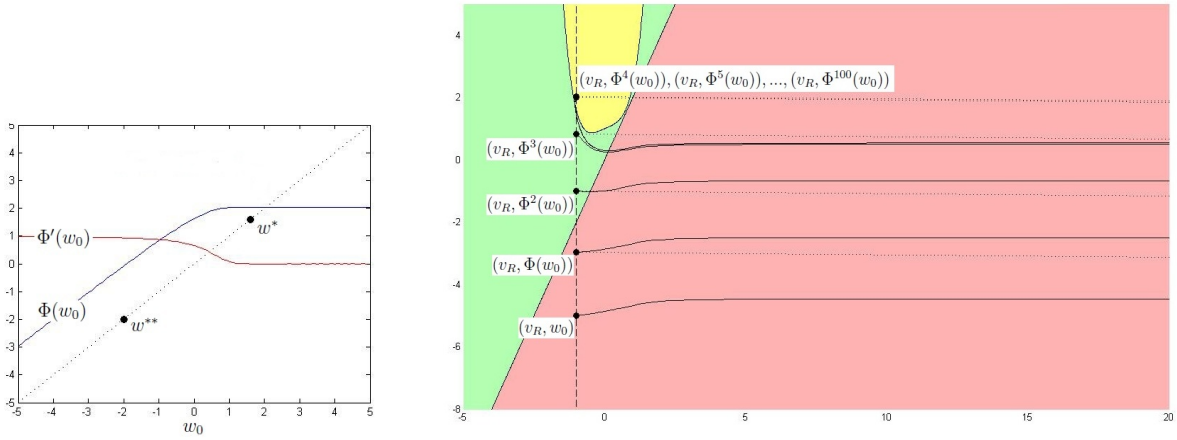

(a) Adaptation map

(b) Numerical solution with initial condition $(-1, -5)$ and 100 spiking events; resetting portrayed by the dotted lines

Figure 5.2: Quartic model

that $F'(v_R) + F'(w_T/b) \approx -3.19 < -0.4 = -2a$, and $F(v_R) = (-1)^4 + 2a(-1) = 3.6$, $F(w_T/b) \approx 0.05$ so that $F(v_R) \geq F(w_T/b)$. Therefore, Theorem 4.4.4 applies and it follows that all initial conditions on the reset line lead to regular spiking.

5.2 Exponential model

Now, consider the model (4.1) with $F(v) = e^v - v$. This is the exponential model introduced by Brette and Gerstner in [2]. Taking parameter values $b = 5/3$, $I = 0$ and $v_R = -3$ gives the phase plane shown in Figure 5.1(b); parameter values are chosen to illustrate the application of Theorem 4.4.4. It can be checked that the vector field has no critical points.

Let $a = 0.05$. Taking $d = 1.5$ and $v_S = \infty$ gives the adaptation map shown in Figure 5.3(a). Observe that $|\Phi'(w_0)| < 1$ on the subset of its domain shown in the figure. Taking the initial condition $w_0 = -5$ on the reset line gives the solution shown in Figure 5.3(b) which appears to converge to a regular spiking pattern. To check that all initial conditions lead to regular spiking, it suffices to verify the conditions of Theorem 4.4.4. We compute $ab = 1/12 < 1$ and $F'(v_R) = e^{-3} - 1 \approx -0.95 < -0.05 = -a$. Then, v_T satisfies $F'(v_T) = 0$ or $e^{v_T} - 1 = 0$, so that $v_T = 0$, and $w_T = F(v_T) = 1$. $F'(w_T/b) = e^{3/5} - 1 \approx 0.82$, so that $F'(v_R) + F'(w_T/b) \approx -0.13 < -0.1 = -2a$ and $F(v_R) = e^{-3} - (-3) \approx 3.05$, $F(w_T/b) = e^{3/5} - 3/5 \approx 1.22$ so that $F(v_R) \geq F(w_T/b)$ and the conditions of Theorem 4.4.4 are satisfied. It follows that all initial conditions

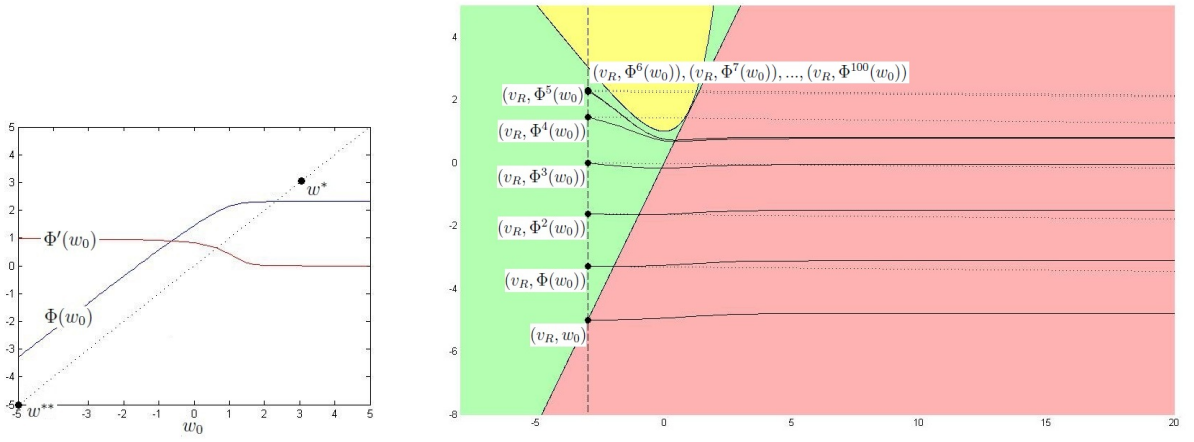

(a) Adaptation map

(b) Numerical solution with initial condition $(-3, -5)$ and 100 spiking events; resetting portrayed by the dotted lines

Figure 5.3: Exponential model

on the reset line lead to regular spiking.

Note that for this model, the slope of $F(v)$ rises sharply to the right of v_T, and goes monotonically towards -1 to the left of v_T, therefore the condition $F'(v_R) + F'(w_T/b) < -2a$ is difficult to satisfy. This is why in this example the v-nullcline and w-nullcline are taken so close to one another.

5.3 Izhikevich Model

Take now the model (4.1) with $F(v) = 0.04v^2 + 5v + 140$. This is known as the Izhikevich model [11]. Take the parameter values $I = 0$, $a = 0.005$, $b = 0.265$, $v_R = -65$, $v_S = 30$, and $d = 1.5$, which are used in [17] in simulations of the effect of deep brain stimulation on a network of neurons. This gives the phase plane shown in Figure 5.4, where the vector field has two critical points, denoted v_- and v_+ where $v_- < v_+$. For this model the domain of the adaptation map is the whole real line, that is, all initial conditions on the reset line lead to a spiking event (this can be checked via the method described in [22], Section 2.2).

A table of numerical values for this example is given below. Note that $w_T = F(v_T)$ and that $F(v_T)$ is the unique minimum for F. The values given for v_- and v_+ are approximate.

The adaptation map is shown in Figure 5.5(a), and a numerical solution of the model is depicted in Figure 5.5(b). Solution curves for one hundred spiking events

v_R	-65
w^*	-16
w^{**}	-17.225
v_T	-62.5
w_T	-16.25
v_-	-60.97
v_+	-57.41

Table 5.1: Table of values for the Izhikevich model with parameters described at the beginning of Section 5.3

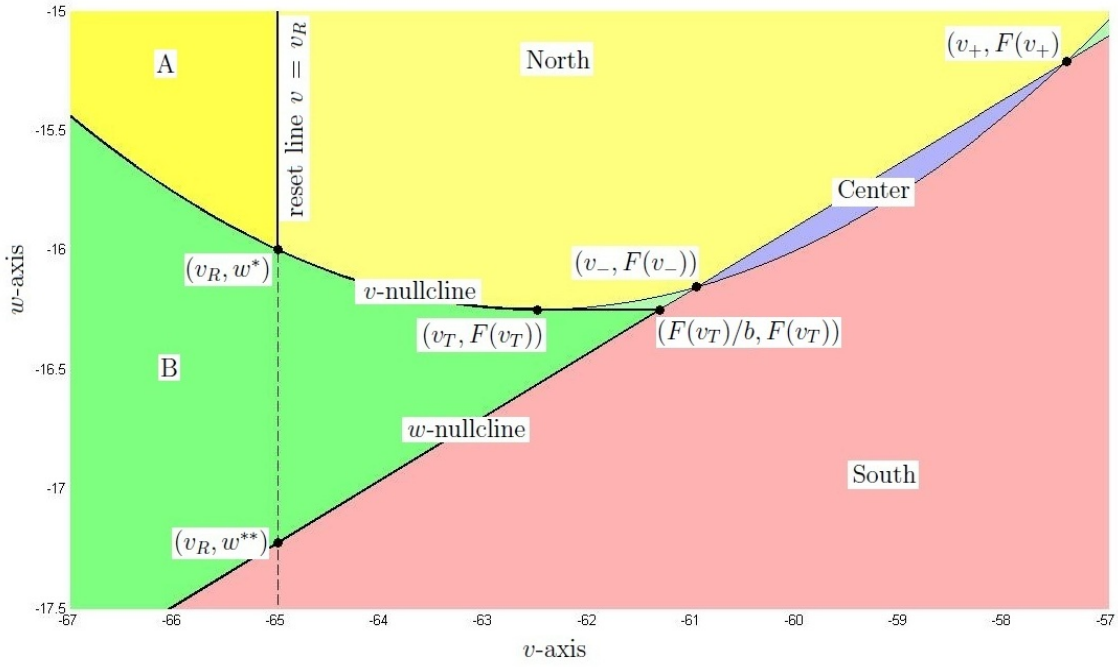

Figure 5.4: Phase plane for the Izhikevich model

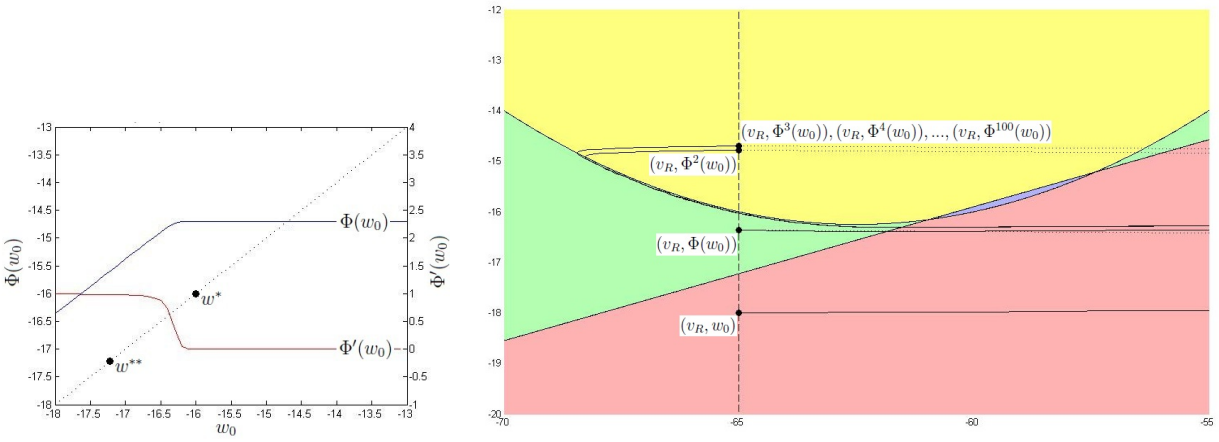

(a) Adaptation map

(b) Numerical solution with initial condition $(-65, -18)$ and 100 spiking events; resetting portrayed by the dotted lines

Figure 5.5: Izhikevich model

are shown; after the third spike, subsequent solution curves are indistinguishable, therefore it appears that the solution is converging to a regular spiking behaviour. We want to prove that this is the case for all initial conditions, therefore our goal in this section is to prove the following theorem.

Theorem 5.3.1. *All initial conditions on the reset line lead to regular spiking.*

As discussed in Section 4.1, to show that regular spiking occurs, we need to show that all orbits under Φ converge to a unique fixed point. The proof consists of two parts.

1. It is shown that all orbits under Φ eventually enter and remain in (w^*, ∞).

2. It is shown that the contraction integral (4.20) is negative for all path segments with initial point on the reset line above w^*, which implies that Φ is non-expansive on (w^*, ∞).

The result then follows from the discussion in Section 4.1. We begin the proof with Part 1.

Proposition 5.3.2. *Given $w_0 \in \mathbb{R}$, $\exists N \in \mathbb{N}$ such that for $n \geq N$, $\Phi^n(w_0) \in (w^*, \infty)$.*

Proof. First we show that $\Phi((w^*, \infty)) \subset (w^*, \infty)$. It is enough to show for $w_0 > w^*$ that all paths beginning on (v_R, w_0) intersect the w-nullcline above $w^* - d$. Recall that w^{**} denotes the intersection of the reset line with the w-nullcline, that is, $w^{**} = bv_R$.

Draw the line that has slope -0.1 and intersects the point (v_R, w^{**}). On this line, $\partial_v(g/f) = 0$ gives a quadratic equation in v. It can be checked by computation that this equation has two roots, one on either side of $v = -65$, and that $\partial_v(g/f) > 0$ when $v = -65$, which implies that the lesser root is a minimum of g/f. At this root, g/f is greater than -0.1, which implies that trajectories cross the line from the left. In particular, since $w^* = -16$ and $w^{**} = -17.225$, trajectories starting on the reset line above w^* must intersect the w-nullcline at a w value that is greater than $w^{**} > w^* - d$, and since $w' > 0$ below the w-nullcline, these trajectories are reset to a w-value that is greater than w^*.

Observe for $w_0 < w^{**}$ that $\Phi(w_0) \geq w_0 + d$ since w' is positive everywhere below the w-nullcline. Thus for any $w_0 \in \mathbb{R}$ there exists an N such that $\Phi^N(w_0) > w^{**}$. Since $\Phi(w^{**}) \geq w^{**} + d > w^*$ it follows that $\Phi^{N+1}(w_0) > w^*$. Then $\Phi(w^*, \infty) \subset (w^*, \infty)$ implies that $\Phi^n(w_0) > w^*$ for all $n \geq N + 1$. □

Part 1 is proved. In the next three propositions, we address Part 2. We are interested in trajectories $\phi(r, x_0)$ with $x_0 = (v_R, w_0)$ and $w_0 > w^*$. We want to show that

$$\int_0^{r_W} G(\phi(s, x_0)) + H(\phi(s, x_0)) + J(\phi(s, x_0))ds + \int_{r_W}^{r_S} L_V(\phi(s, x_0))ds < 0$$

This is the contraction integral in (4.20) expressed with the notation from (4.23). The following proposition proves that the first two terms are negative.

Proposition 5.3.3. *The terms $\int_0^{r_W} G(\phi(s, x_0))ds$ and $\int_0^{r_W} H(\phi(s, x_0))ds$ in the above integral are negative.*

Proof. Here $ab < 1$, $F'(v_R) = -0.2 < -a$ and $F'(v_R) + F'(w_T/b) \approx -0.11 < -2a$ so that the results of Proposition 4.4.2 hold. Also, $F(v)$ is symmetric, since it is quadratic, and $v_R + w_T/b \approx -126.32 < -125 = 2v_T$ and so the results of Proposition 4.4.3 hold (see the remark following Proposition 4.4.3). The result follows from these two propositions. □

Consider now the term $\int_{r_W}^{r_S} L_V(\phi(s, x_0))ds$. Since the model has two critical points, Proposition 4.4.1 does not apply. Indeed, L_V is positive if and only if

$$g = a(bv - w) > a(F(v) - w + I) = af$$

that is, when $bv > F(v) + I$, which is true on the strip $\{(v, w) : v_- < v < v_+\}$ and nowhere else. Therefore

$$\int_{v_-}^{v_+} \frac{g - af}{f^2} dv$$

understood as an integral along trajectories is an upper bound on $\int_{r_W}^{r_S} L_V(\phi(s, x_0))ds$. To show the contraction integral is negative it suffices to show that

$$\int_0^{r_W} J(\phi(s, x_0))ds + \int_{v_-}^{v_+} \frac{g - af}{f^2} dv < 0$$

As mentioned in Section 4.4, J is everywhere negative. We estimate both integrals, and show that the negative contribution outweighs the positive contribution. We begin with the positive contribution.

Proposition 5.3.4.

$$\int_{v_-}^{v_+} \frac{g - af}{f^2} dv < 1.5 \times 10^{-3} \tag{5.1}$$

Proof. Since $f > 0$ in the South region, $\partial_w \frac{g-af}{f^2} = \frac{2(g-af)}{f^3} > 0$ and $g - af > 0$ on (v_-, v_+). To bound the integral in (5.1) it suffices to evaluate it along a curve that lies above trajectories on the strip $\{(v, w) : v_- < v < v_+\}$. We construct the curve depicted in Figure 5.6, and estimate the integral in (5.1) along this curve.

In Section 4.4 it is shown that trajectories lie in $A \cup B$ up to the w-nullcline, therefore when $v = w_T/b$ trajectories have $w < w_T$. Also, $g/f < a$ whenever the v-nullcline lies above the w-nullcline, that is, when $v \notin [v_-, v_+]$. Therefore, the line that has slope a and intersects $(w_T/b, w_T)$ lies above trajectories on the set $w_T/b \leq v \leq v_-$. Then, take another line that intersects the first line at $v = v_-$ and has slope $2a$. It can be checked that $g/f < 2a$ on this line for $v_- \leq v \leq v_+$, so that trajectories do not cross it from below. Together these lines give an upper bound curve. Discretizing the expression in (5.1) and evaluating it numerically along this upper bound curve gives the bound 1.5×10^{-3} on the integral in (5.1). □

We now estimate the negative contribution.

Proposition 5.3.5.

$$\int_0^{r_W} J(\phi(s, x_0))dr < -1.5 \times 10^{-3} \tag{5.2}$$

Proof. The approach is to identify a region through which trajectories pass, and to estimate the integral in that region. Specifically, we carve out the channel C shown

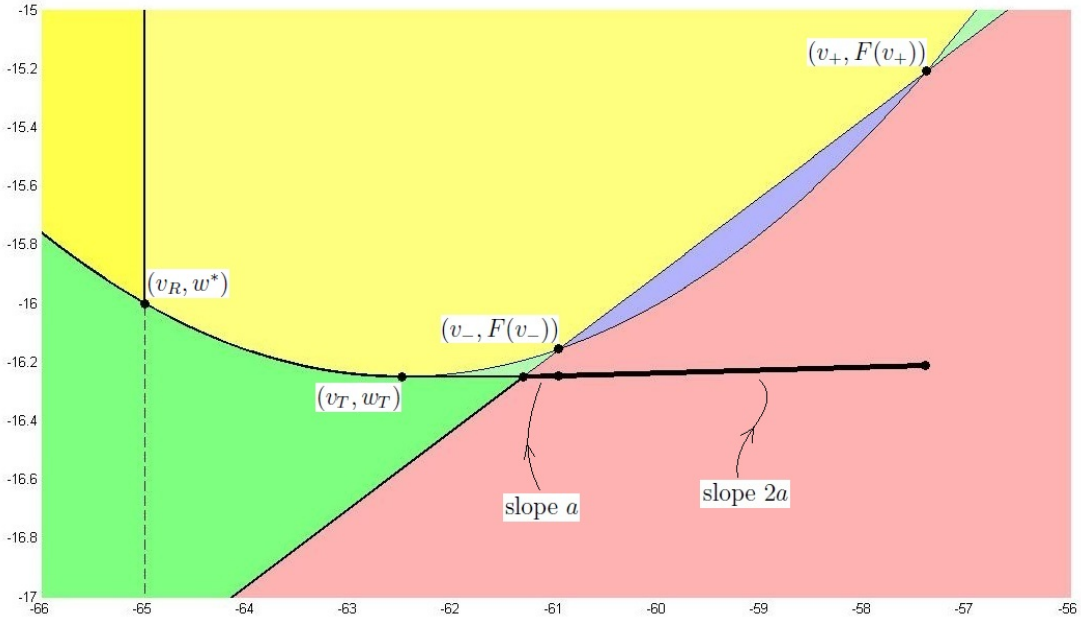

Figure 5.6: Upper bound curve for path segments, for $v \in [v_-, v_+]$

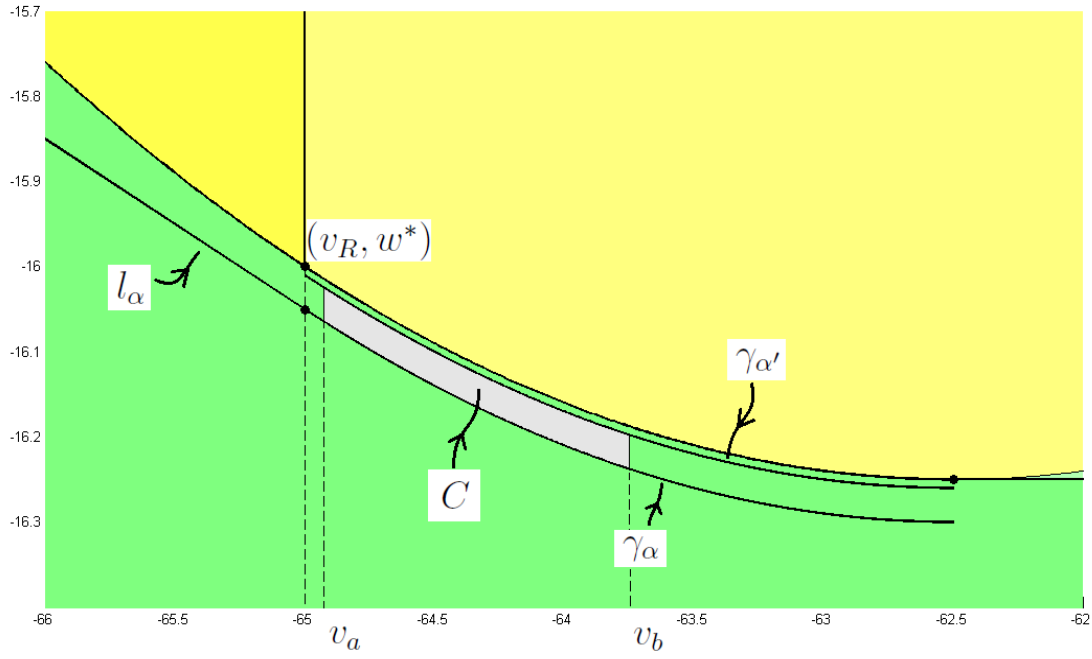

Figure 5.7: The channel C

in Figure 5.7 and prove that the inequality

$$\int_{\{0\le r\le r_W\,:\,\phi(r,x_0)\in C\}} J(\phi(s,x_0))ds < -1.5\times 10^{-3}$$

holds for each trajectory. Since J is everywhere negative this implies (5.2).

In the figure there are two curves γ_α and $\gamma_{\alpha'}$ that lie parallel to the v-nullcline, and a line l_α which is the tangent line to γ_α at $v = v_R$. The channel consists of the region bounded above by $\gamma_{\alpha'}$, below by γ_α, on the left by $v_a = -64.925$ and on the right by $v_b = -63.75$. We proceed as follows.

1. For $v \le v_b$ we show that trajectories lie above $\gamma_\alpha \cup l_\alpha$.

2. For $v_a \le v \le v_b$ we show that trajectories lie below $\gamma_{\alpha'}$.

3. We estimate the integral of J for trajectories in the channel.

We begin with Step 1. Take the curve γ_α that lies a distance $\alpha = 0.05$ below the v-nullcline, and take l_α, its tangent line at $v = v_R$, which has slope -0.2. On l_α, $\partial_v(g/f)$ gives a quadratic equation in v that has two roots, one on either side of v_R. Also, $\partial_v(g/f) > 0$ at v_R, so that the lesser root is a minimum of g/f. The value

of g/f at this root is greater than -0.2, therefore trajectories cross l_α from the left. Now, γ_α has slope F', since it lies parallel to the v-nullcline, and along γ_α, f takes the value α, and g and F' both increase with v. Therefore g has its minimum at v_R, and F' has its maximum at $v = v_b$, and it can be checked that

$$\max_{[v_R,v_b]} F'(v) = F'(v_b) < g(v_R)/\alpha = \min_{[v_R,v_b]} g/f$$

Therefore, for $v_R \le v \le v_b$, γ_α is crossed from below, so that together, l_α and γ_α give a lower bound on trajectories for $v \le v_b$.

Now, we show Step 2. For $\alpha' = 0.01$ take the curve $\gamma_{\alpha'}$ that lies a distance α' below the v-nullcline. On this curve $g/f = -0.6075$ at v_R, and $g/f = -0.3369$ at v_b, and along it f is constant and $|g|$ decreases in the v direction at least up to v_b, thus $g/f \in [-0.6075, -0.3369]$ on $\gamma_{\alpha'}$, for $v \in [v_R, v_b]$. Also, $F'(v_R) = -0.2$, $F'(v_b) = -0.1$, and F' increases with v, therefore the slope of $\gamma_{\alpha'}$ takes values in $[-0.2, -0.1]$. It follows that trajectories cross $\gamma_{\alpha'}$ from above. For $v_R \le v \le v_b$ the trajectory with initial point (v_R, w^*) is an upper bound. Draw the line that has slope $-1/3$ and intersects (v_R, w^*). Between $\gamma_{\alpha'}$ and the v-nullcline trajectories have slope at most $-0.3369 < -1/3$ and so this line is not crossed before $\gamma_{\alpha'}$. Therefore, the intersection of the two lines gives a left-hand bound on the channel. To estimate this intersection draw the tangent line to $\gamma_{\alpha'}$ at v_R, which has slope -0.2. The two lines have initial separation $\alpha' = 0.01$ and so they intersect after a distance $0.01/(-0.2 - (-1/3)) = 0.075$. Since $v_a = -65 + 0.075 = -64.925$, then for $v_a \le v \le v_b$ path segments lie between γ_α and $\gamma_{\alpha'}$.

Now, we give Step 3. We want to show that

$$\int_{v_a}^{v_b} \frac{-f^2 a}{(f^2+g^2)^{3/2}} \frac{dt}{dv} dv = \int_{v_a}^{v_b} \frac{-a}{|f|(1+(g/f)^2)} dv < -1.5 \times 10^{-3} \tag{5.3}$$

along trajectories contained in C. On C, $1/|f| \ge 1/\alpha = 20$ and $|g/f| < 1$, so the integral in (5.3) is less than

$$(v_b - v_a)\frac{-a}{2\alpha} = -0.059$$

which is less than -1.5×10^{-3}. □

We have shown that the contraction integral in (4.20) is negative, from which it follows that Φ is non-expansive on (w^*, ∞). Since all orbits under Φ are eventually

contained in (w^*, ∞) it follows that all orbits under Φ converge to a unique fixed point, so that all initial conditions lead to regular spiking. This concludes the proof of Theorem 5.3.1.

Remark 3. *For the example of the Izhikevich model, $\Phi(w^*) > w^*$ and $\Phi^2(w^*) > w^*$ as shown in Figure 5.5. From Theorem 3.3 of [22] it follows that all orbits under Φ converge either to a unique fixed point or to a periodic orbit of period 2. Therefore the result of Theorem 5.3.1 is a refinement of that result which is biologically relevant, since regular spiking and period 2 bursting are functionally different behaviours. Also, the above proof shows how stability can be verified by measuring the separation of orbits in the phase plane, without computing the orbits directly; in this case a Riemann sum in Proposition 5.1 is the only computer-assisted computation.*

Chapter 6

Discussion and Conclusions

The adaptive integrate-and-fire (AIF) model has a rich spiking dynamics, and can be accurately fitted to recordings of biological neurons. Its dynamics are well-studied both experimentally and analytically. The adaptation map defined in Chapter 4 is an effective description of the spiking behaviour of the model, and its relationship to the subthreshold dynamics of the model has been previously studied.

The transverse local Lyapunov exponent (TLLE), defined in Chapter 4, describes the local rate of separation of orbits on the phase plane. Relating this information to the adaptation map gives a sufficient condition for the stability of regular spiking in terms of a path integral along trajectories. Exploiting the form of the AIF model, estimation of this integral leads to a sufficient condition for the stability of regular spiking, in terms of the model parameters.

In existing literature, in particular in [22], sufficient conditions for regular spiking are given in terms of the behaviour of the adaptation map. Using a TLLE, in Theorem 4.4.4 sufficient conditions are given directly in terms of the model parameters. The method described in Chapter 4 applies to any differentiable dynamical system in 2 or more dimensions; for example, the TLLE with respect to a chosen orthogonal field can always be defined. For the AIF model this method leads to a biologically relevant result, since it distinguishes between regular spiking and period 2 bursting in certain cases.

The method described in Section 4.3 of this thesis may be applied to more general neuron models in a number of ways. For the AIF model, possible generalizations

include a time-dependent input current $I(t)$. The stability of regular spiking might be established in situations where the time average of $I(t)$ is such that on average, orbits still converge towards one another. Also, even in regions of parameters not covered by Theorem 4.4.4 there appears to be a strong contraction of orbits in the phase plane. Therefore, with additional work the region of parameters described by Theorem 4.4.4 might be extended by taking into account some additional contraction of the orbits that was not exploited in the proof of that theorem. Also, the results of section 4.3 concerning the TLLE generalize easily to higher dimensions. Similar result may be therefore obtained for a small network of AIF neurons, for example. A similar approach to the one used for a single neuron can be used, in which contraction of orbits in a (higher-dimensional) phase space is measured.

The present method is limited by the ability of the user to estimate the TLLE along a (possibly more complicated) trajectory in phase space. In this thesis, the estimation is helped by some useful algebraic properties of the expression for the TLLE as exploited in Section 4.4 that may not be available in general. Since the method is a method of stability analysis, it is not well suited to proving the existence of more complicated spiking behaviour.

Finally, the method may find application in more general ODE models not related to neuronal dynamics. For example, the method may be useful for calculating the Lyapunov exponent of a chaotic attractor by defining a return map on a cross-section of the phase space, and then applying the method to measuring the separation of orbits from a starting point on the cross-section, until the first return to that cross-section. The use of a well-chosen transverse component of the displacement may lead to a convenient expression for the derivative of the return map, as was the case in this thesis.

Bibliography

[1] L. Badel, S. Lefort, R. Brette, C.C. Petersen, W. Gerstner, and M.J. Richardson. Dynamic I-V curves are reliable predictors of naturalistic pyramidal-neuron voltage traces. *J. Neurophysiol.*, 99:656–666, 2008.

[2] R. Brette and W. Gerstner. Adaptive exponential integrate-and-fire model as an effective description of neuronal activity. *J. Neurophysiol.*, 94:3637–3642, 2005.

[3] C. Clopath, R. Jolivet, A. Rauch, H.R. Lüscher, and W. Gerstner. Predicting neuronal activity with simple models of the threshold type: Adaptive exponential integrate-and-fire model with two compartments. *Neurocomput.*, 70:1668–1673, 2007.

[4] S. Coombes and P.C. Bressloff. Mode locking and Arnold tongues in integrate-and-fire neural oscillators. *Physical Review E*, 60:2086–2096, 1999.

[5] B. Eckhardt and D. Yao. Local Lyapunov exponents in chaotic systems. *Physica D*, 65:100–108, 1993.

[6] G.B. Ermentrout and D.H. Terman. *Mathematical Foundations of Neuroscience*. Springer, 2010.

[7] G. Haubs and H. Haken. Quantities describing local properties of chaotic attractors. *Z. Phys. B*, 59:459–468, 1985.

[8] R. Hermann. *Differential geometry and the calculus of variations*. Academic Press, 1968.

[9] A.V. Hill. Excitation and accomodation in nerve. *Proc. Roy. Soc. B*, 119:305–355, 1936.

[10] A. L. Hodgkin and A. F. Huxley. A quantitative description of membrane current and its application to conduction and excitation in nerve. *Journal of Physiology*, 117:500–544, 1952.

[11] E. Izhikevich. Simple model of spiking neurons. *IEEE Trans. Neural Networks*, 14:1569–1572, 2003.

[12] E. Izhikevich. *Dynamical Systems in Neuroscience*. MIT Press, 2007.

[13] B.W. Knight. Dynamics of encoding in a population of neurons. *J. Gen. Physiol.*, 59:734–766, 1972.

[14] L. Lapicque. Recherches quantitatives sur l'excitation électrique des nerfs traitée comme une polarization. *J. Physiol. Path. Gen.*, 9:620–635, 1907.

[15] W. Lohmiller and J.-J. E. Slotine. On contraction analysis for non-linear systems. *Automatica*, 34:683–696, 1998.

[16] R.K. Miller and A.N. Michel. *Ordinary Differential Equations*. Academic Press, 1982.

[17] J. Modolo, J. Henry, and A. Beuter. Dynamics of the subthalamo-pallidal complex in Parkinson's disease during deep brain stimulation. *J. Biol. Phys.*, 34:351–366, 2008.

[18] J.M. Nese. Quantifying local predictability in phase space. *Physica D*, 35:237–250, 1989.

[19] R. Stein. A theoretical analysis of neuronal variability. *Biophys. J.*, 5:173–194, 1965.

[20] J. Touboul. Bifurcation analysis of a general class of nonlinear integrate-and-fire neurons. *SIAM J. Appl. Math.*, 68:1045–1079, 2008.

[21] J. Touboul and R. Brette. Dynamics and bifurcations of the adaptive exponential integrate-and-fire model. *Biol. Cybern.*, 99:319–334, 2008.

[22] J. Touboul and R. Brette. Spiking dynamics of bidimensional integrate-and-fire neurons. *SIAM J. Applied Dynamical Systems*, 8:1462–1506, 2009.